July/August 2020
www.arrl.org

QEX

A Forum for Communications Experimenters

Issue No. 321

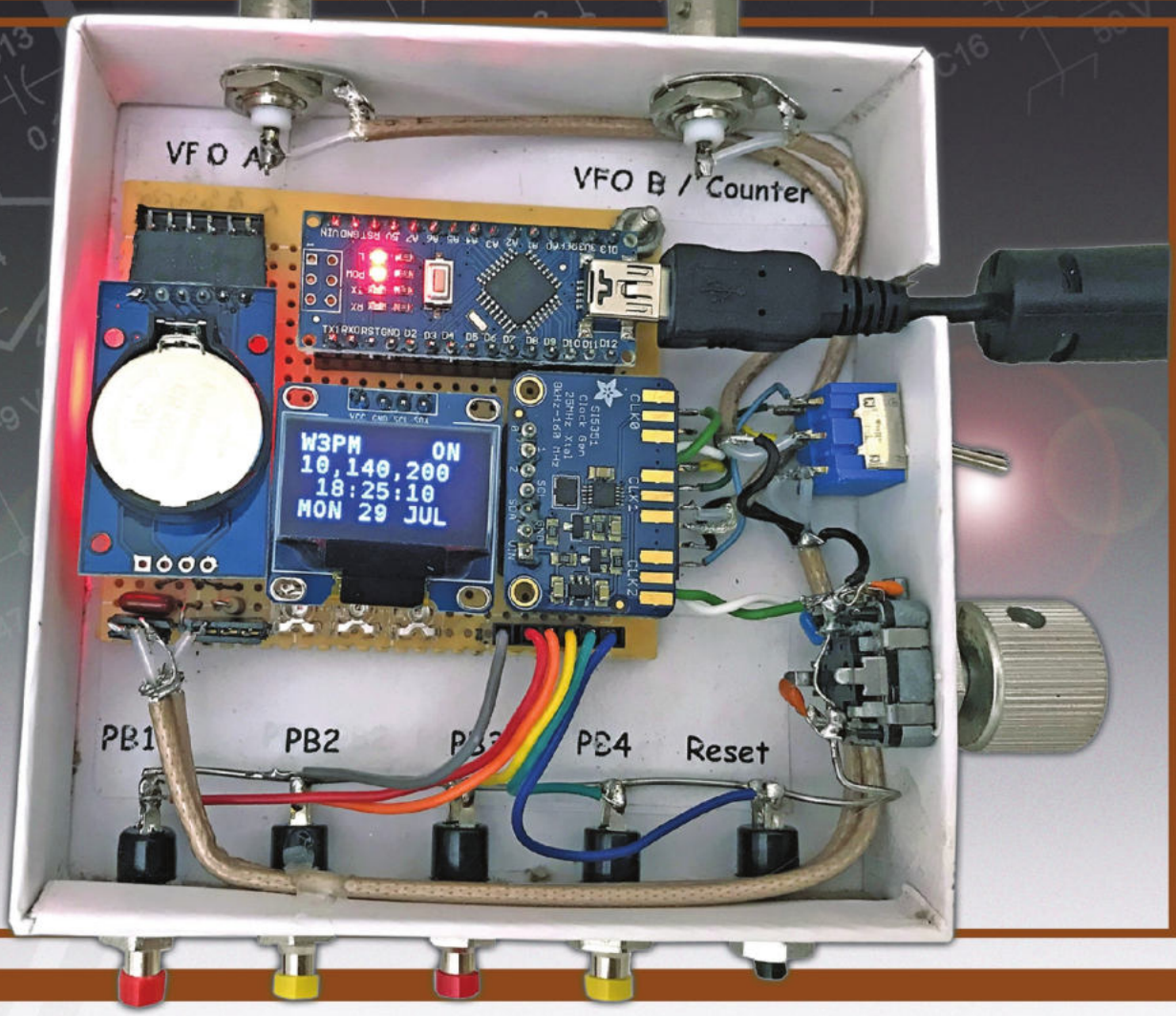

W3PM/GM4YRE builds a menu-driven multifunction project.

APRS® / D-STAR®

TH-D74A 144/220/430 MHz Tribander

The TH-D74A represents the ultimate in APRS and D-STAR performance. KENWOOD has already garnered an enviable reputation with the TH-D72A handheld APRS amateur radio transceiver. Now it has raised the bar even further with the TH-D74A, adding support for D-STAR, the digital voice & data protocol developed by the JARL, and enabling simultaneous APRS and D-STAR operation – an industry first.

- APRS compliance using packet communication to exchange real-time GPS position information and messages
- Compliant with digital/voice mode D-STAR digital amateur radio networks
- Built-in high performance GPS unit with Auto Clock Setting
- Wide-band and multi-mode reception
- 1.74" (240 x 180 pixel) Transflective color TFT display
- IF Filtering for improved SSB/CW/AM reception
- High performance DSP-based audio processing & voice recording
- Compliant with Bluetooth, microSD & Micro-USB standards
- External Decode function (PC Decode 12kHz IF Output, BW:15 kHz)
- Free software for Memory and Frequency Control Program
- Data Import / Export (Digital Repeater List, Call sign, Memory Channel)
- Four TX Power selections (5/2/0.5/0.05 W)
- Dust and Water resistant IP54/55 standards

APRS (The Automatic Packet Reporting System) is a registered American trademark of WB4APR (Mr. Bob Bruninga). D-Star is a digital radio protocol developed by JARL (Japan Amateur Radio League).

KENWOOD

Customer Support/Distribution Customer Support:
(310) 639-4200 Fax: (310) 537-8235

www.kenwood.com/usa

ISO9001 Registered

ADS#38619

QEX

July/August 2020

QEX (ISSN: 0886-8093) is published bimonthly in January, March, May, July, September, and November by the American Radio Relay League, 225 Main St., Newington, CT 06111-1494. Periodicals postage paid at Hartford, CT and at additional mailing offices.

POSTMASTER: Send address changes to: QEX, 225 Main St., Newington, CT 06111-1494 Issue No. 321

Publisher
American Radio Relay League

Kazimierz "Kai" Siwiak, KE4PT
Editor

Lori Weinberg, KB1EIB
Assistant Editor

Scotty Cowling, WA2DFI
Ray Mack, W5IFS
Contributing Editors

Production Department

Steve Ford, WB8IMY
Publications Manager

Michelle Bloom, WB1ENT
Production Supervisor

David Pingree, N1NAS
Senior Technical Illustrator

Brian Washing
Technical Illustrator

Advertising Information Contact:

Janet L. Rocco, W1JLR
Business Services
860-594-0203 – Direct
800-243-7768 – ARRL
860-594-4285 – Fax

Circulation Department

Cathy Stepina, *QEX Circulation*

Offices

225 Main St., Newington, CT 06111-1494 USA
Telephone: 860-594-0200
Fax: 860-594-0259 (24 hour direct line)
e-mail: **qex@arrl.org**

Subscription rate for 6 issues:

In the US: $29;

US by First Class Mail: $40;

International and Canada by Airmail: $35

Members are asked to include their membership control number or a label from their *QST* when applying.

In order to ensure prompt delivery, we ask that you periodically check the address information on your mailing label. If you find any inaccuracies, please contact the Circulation Department immediately. Thank you for your assistance.

About the Cover

Gene Marcus, W3PM/GM4YRE, builds an auto-calibrating menu-driven multifunction project that includes a band switched two channel 110 kHz to 112.5 MHz VFO, a band switched 6 m to 2200 m WSPR source, a 6.5 MHz frequency counter, and a clock that displays time, date, and temperature. Frequency and time accuracy are maintained by a highly accurate temperature compensated DS3231 real time clock board. All of these individual project building blocks are combined into one multi-function box controlled by an Arduino Nano or Uno micro-controller.

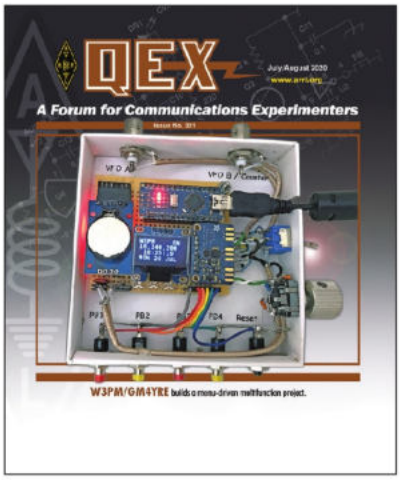

In This Issue

Index of Advertisers

The American Radio Relay League

The American Radio Relay League, Inc, is a noncommercial association of radio amateurs, organized for the promotion of interest in Amateur Radio communication and experimentation, for the establishment of networks to provide communications in the event of disasters or other emergencies, for the advancement of the radio art and of the public welfare, for the representation of the radio amateur in legislative matters, and for the maintenance of fraternalism and a high standard of conduct.

ARRL is an incorporated association without capital stock chartered under the laws of the state of Connecticut, and is an exempt organization under Section 501(c)(3) of the Internal Revenue Code of 1986. Its affairs are governed by a Board of Directors, whose voting members are elected every three years by the general membership. The officers are elected or appointed by the Directors. The League is noncommercial, and no one who could gain financially from the shaping of its affairs is eligible for membership on its Board.

"Of, by, and for the radio amateur," ARRL numbers within its ranks the vast majority of active amateurs in the nation and has a proud history of achievement as the standard-bearer in amateur affairs.

A *bona fide* interest in Amateur Radio is the only essential qualification of membership; an Amateur Radio license is not a prerequisite, although full voting membership is granted only to licensed amateurs in the US.

Membership inquiries and general correspondence should be addressed to the administrative headquarters:

ARRL
225 Main St.
Newington, CT 06111 USA
Telephone: 860-594-0200
FAX: 860-594-0259 (24-hour direct line)

Officers

President: Rick Roderick, K5UR
P.O. Box 1463, Little Rock, AR 72203

The purpose of *QEX* is to:

1) provide a medium for the exchange of ideas and information among Amateur Radio experimenters,

2) document advanced technical work in the Amateur Radio field, and

3) support efforts to advance the state of the Amateur Radio art.

All correspondence concerning *QEX* should be addressed to the American Radio Relay League, 225 Main St., Newington, CT 06111 USA. Envelopes containing manuscripts and letters for publication in *QEX* should be marked Editor, *QEX*.

Both theoretical and practical technical articles are welcomed. Manuscripts should be submitted in word-processor format, if possible. We can redraw any figures as long as their content is clear. Photos should be glossy, color or black-and-white prints of at least the size they are to appear in *QEX* or high-resolution digital images (300 dots per inch or higher at the printed size). Further information for authors can be found on the Web at **www.arrl.org/qex/** or by e-mail to **qex@arrl.org**.

Kazimierz "Kai" Siwiak, KE4PT

Perspectives

An Expanded *QEX* Audience

We noted previously in this column that *QEX* Online edition is available to all ARRL members as a benefit. Members and non-members can still subscribe to the *printed* edition of *QEX* at the usual subscription rates. As a member benefit, the whole suite of ARRL online e-magazines is at your disposal. What this means for *QEX* is a potentially greatly expanded readership that includes all ARRL members plus the non-members who subscribe to the *QEX* printed edition. We recognize that the expanded membership profile boasts individuals from all walks of life and at all levels of technical expertise, not just engineers and technologists.

Keep the detailed and high technical level articles coming in, even though they may appear as *'mathematica obscurata'* to many of our new readers. To help transition those for whom engineering and technology are not their primary language, and as a hearty welcome to *QEX*, we shall embark on a self-paced series of essays in electrical engineering designed by Eric Nichols, KL7AJ. The essays will cover many of the fundamental topics that one would encounter in a university-level electrical engineering curriculum. We want this to be a highly interactive essay series, so we strongly encourage your feedback about the draft outline of the essays, and also about topics that you would want us to cover. We will do our best to accommodate you.

In This Issue

Steve Franke, K9AN; Bill Somerville, G4WJS; and Joe Taylor, K1JT, describe the FT4 and FT8 digital modes implemented in *WSJT-X*.

Gene Marcus, W3PM/GM4YRE, builds a project that includes a two-channel VFO, WSPR source, frequency counter, and a clock.

Eric Nichols, KL7AJ, presents Part 2 of his Double Balanced Mixer series.

Steve Stearns, K6OIK, explores general uniform transmission lines having complex characteristic impedance and propagation constant.

QEX introduces a self-paced essay series in electrical engineering designed by Eric Nichols, KL7AJ.

Writing for *QEX*

Please keep the full-length *QEX* articles flowing in, or share a **Technical Note** of several hundred words in length plus a figure or two. Let us know that your submission is intended as a **Note**. *QEX* is edited by Kazimierz "Kai" Siwiak, KE4PT, (**ksiwiak@arrl.org**) and is published bimonthly. The content is driven by you, the reader and prospective author. *QEX* is a forum for the free exchange of ideas among communications experimenters. All ARRL members can enjoy the *QEX* Online edition as a member benefit. The printed edition annual subscription rate (six issues per year) for members and non-members is $29 in the United States. First-Class mail delivery in the US is available at an annual rate of $40. For international subscribers, including those in Canada and Mexico, *QEX* printed edition can be delivered by airmail for $35 annually, see **www.arrl.org/qex**.

Would you like to write for *QEX*? We pay $50 per published page for full articles and *QEX* Technical Notes. Get more information and an Author Guide at **www.arrl.org/qex-author-guide**. If you prefer postal mail, send a business-size self-addressed, stamped (US postage) envelope to: *QEX* Author Guide, c/o Maty Weinberg, ARRL, 225 Main St., Newington, CT 06111.

Very kindest regards,

Kazimierz "Kai" Siwiak, KE4PT

QEX Editor

Gene Marcus, W3PM, GM4YRE

113 Wickerberry Lane, Madison, AL 35756; **w3pm@arrl.net**

Simple and Inexpensive Auto-Calibrating Multifunction Project

The project includes a two-channel VFO, WSPR source, frequency counter, and a clock.

This menu-driven multifunction project includes a band switched two channel 110 kHz to 112.5 MHz VFO, band switched 6 m to 2200 m WSPR source, a 0 to 6.5 MHz frequency counter, and a clock that displays time, date, and temperature. Frequency and time accuracy are maintained by a highly accurate temperature compensated DS3231 real time clock (RTC) board.

This project started with the purchase of a DS3231 RTC to use in a time-critical project. As I became familiar with the functions of this device I realized that it had far more potential than just providing accurate time. I discovered that the internal temperature-stabilized oscillator could be programmed to output a one pulse-per-second (pps) square wave with an uncertainty of about 2 ppm from 0 °C to 40 °C (32 °F to 104 °F). This output could be used as a frequency counter gate to automatically calibrate a Si5351 frequency source to provide accurate frequencies from 8 kHz to more than 112 MHz. An auto-calibrated VFO was shortly in operation, then a WSPR source, followed by a very basic frequency counter, and of course a station clock with day-of-the-week, date, and temperature functions. All of these individual projects were then combined into one multi-function box controlled by single Arduino Nano (or Uno) using one Arduino sketch (the Arduino term for the program).

Figure 1 shows the building blocks for this project that consist of four boards: an Arduino Nano (or Uno) microcontroller, a Si5351A clock generator breakout board, a DS3231 real time clock (RTC) board, and a 0.96-inch 128 × 64 serial I2C OLED display board.

The boards communicate with the Nano microcontroller over an I2C bus using three wires. The boards were chosen because they are highly capable, inexpensive, well documented, and available over the internet from a wide variety of vendors. The completed unit draws little power and can be powered by the Nano microcontroller through the USB cable connected to a computer, a USB charger, or by some 5 V USB battery-backup chargers.

The Building Blocks

The four building block details are as follows.

DS3231SN

Frequency and timing accuracy is provided by the DS3231SN RTC. Be sure your board uses the DS3231SN IC, some vendors substitute the DS3231M version, which is not as accurate as the "N" version. The RTC is re-configured by the sketch for a 1 pps output that is used as a counter gate to calibrate the Si5351A clock generator breakout board. The frequency calibration algorithm is a modified version of the one I used in my July/August, 2015 *QEX* article, "An Arduino Controlled GPS Corrected VFO".

Si5351A

The Si5351A is a very popular clock generator used in many commercial and homebrew projects during the last few years. The Si5351A board does have limitations. Although it is a highly capable and stable board, the output is a square wave with odd harmonic frequencies present in the output. The 7 dBm (5 mW) square-wave output does make a good source for some mixers. Phase noise is also higher than other popular programmable signal sources. A search of the internet will yield a wealth of data concerning the performance of the Si5351A IC.

Excellent library routines are available on the internet to simplify Si5351A frequency programming. Instead, I chose to program the Si5351A PL and MultiSynth functions directly without the use of library routines. The resultant code is very simple compared to other routines, but works quite nicely in this application. I found I could easily program the Si5351A board up to 150 MHz using PLL divider techniques. Unfortunately, PLL divider techniques create glitches each time the frequency is changed. Fixed PLL frequencies using MultiSynth division provide glitch-free tuning, but the frequency range is limited to 112.5 MHz using this method.

I developed the Arduino sketch for a Si5351A using a 25 MHz clock frequency. Minor sketch changes are required to accommodate other clock frequencies.

Arduino Nano (or Uno)

The Arduino Nano is a compact, complete and user friendly microcontroller board. These boards are widely used in robotics, embedded systems, and electronic projects where automation is an essential part of

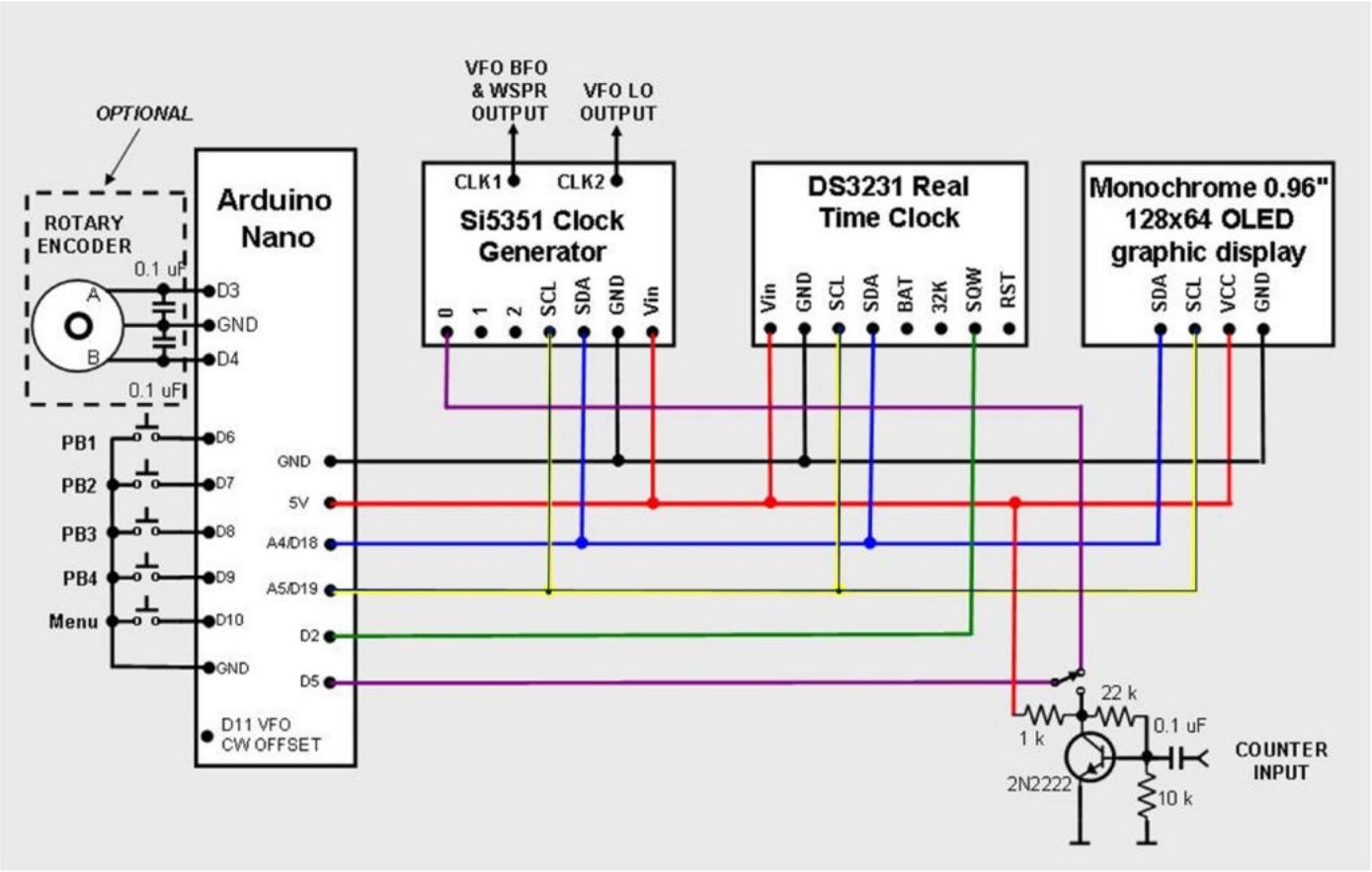

Figure 1 — The schematic diagram shows the optional rotary encoder on the left, and the frequency counter preamplifier / buffer at the lower right.

the system. Based on the ATmega328P processor, it is quite powerful and easy to program using Arduino IDE software. All that is needed is a USB cable to transfer the program from your computer to the board.

OLED Display

The monochrome 0.96 inch 128 × 64 pixel OLED graphic display is very small, but very readable due to the high contrast OLED display. It uses no backlight and draws very little power. Although this is a graphic display, only text data is used in this application.

Options

An optional rotary encoder can also be connected to facilitate frequency changes for VFO operation. Simply wire the encoder as outlined in the schematic. Sketch changes are not required. I used a DigiKey P10859-ND mechanical rotor which is no longer available, however DigiKey does list PEC12R-4217F-N0024 as a substitute.

Construction

Construction of the unit is not critical provided adequate RF techniques are followed. Do not use long unshielded wires for RF and 1 pps connections. I first built the system using a solderless breadboard without any problems. The circuit was then transferred to a piece of perf board and placed in a box with a clear plastic top that I happened to have on hand. Mounting the unit in a metal cabinet is the preferred way to house this project. To improve short and long term accuracy, the unit should be kept at room temperature away from any drafts.

Figure 2 shows my completed unit with the WSPR function selected and band set to 30 meters. I used a discarded box from an Apple TV purchase to house the project. The Si5351A, DS3231SN, and the display are powered from the 5 V pin of the Arduino. You can use the USB programming cable, a separate 5 V dc source connected to the +5 V pin, or a 7 to 12 V dc source connected to the Arduino Nano *Vin* pin to power the unit.

Software Installation and Setup

The Arduino download website **arduino.cc/en/Main/Software** outlines installation instructions for the first-time Arduino user. The Arduino sketch used with this project is available for download from the **www.arrl.org/QEXfiles** and **www.knology.net/~gmarcus/webpages**.

The sketch requires two open source libraries; *SSD1306Ascii* by Bill Greiman (**https://github.com/greiman/SSD1306Ascii**) and *PinChangeInterrupt* by Nico Hood (**https://github.com/NicoHood/PinChangeInterrupt**). Windows users will find the menu bar on top of the active window. Linux and MAC users will find the menu bar at the top of the primary display screen. I found that other more robust ASCII/Graphics libraries were not compatible with the functions and timing complexity of the multifunction sketch.

In the unlikely event of operational problems, I suggest that the builder check the Arduino, OLED display, and RTC boards individually to ensure proper operation. The Arduino board can be checked using some of the example sketches provided with the open source Arduino software. The simple *blink* example sketch will confirm that a sketch can be loaded and the Arduino board is functioning. The OLED display can be checked by running one of the *AvrI2C* examples found with the *SSD1306Ascii* library. The DS3231SN RTC board can be

checked by running a time initialization sketch. A search of the internet will provide a number of methods to initialize the board. Adafruit Industries provides a very good tutorial to confirm that the board is operational. Upon initialization, the time will be a few seconds slow. This is because the time set is the time that the sketch was compiled, not the current time. If WSPR is to be used, the time will have to be updated using the "Clock Set" push buttons after the project is completed. Provided a battery is used with the DS3231, the date will not require setting for a year or more.

Prior to using WSPR, your call sign, grid square locator, power level, transmit offset frequency, and transmit interval will require customization within the sketch. The sketch is fully documented and configuration instructions are found in the WSPR configuration data section near the beginning of the sketch.

There are a number of pre-set frequencies divided into bands within the VFO configuration data section of the sketch. The displayed frequency is arithmetically corrected when both output ports are used in the VFO/LO configuration. Multiple bands can be configured in this manner. Instructions are found in the sketch if changes are required.

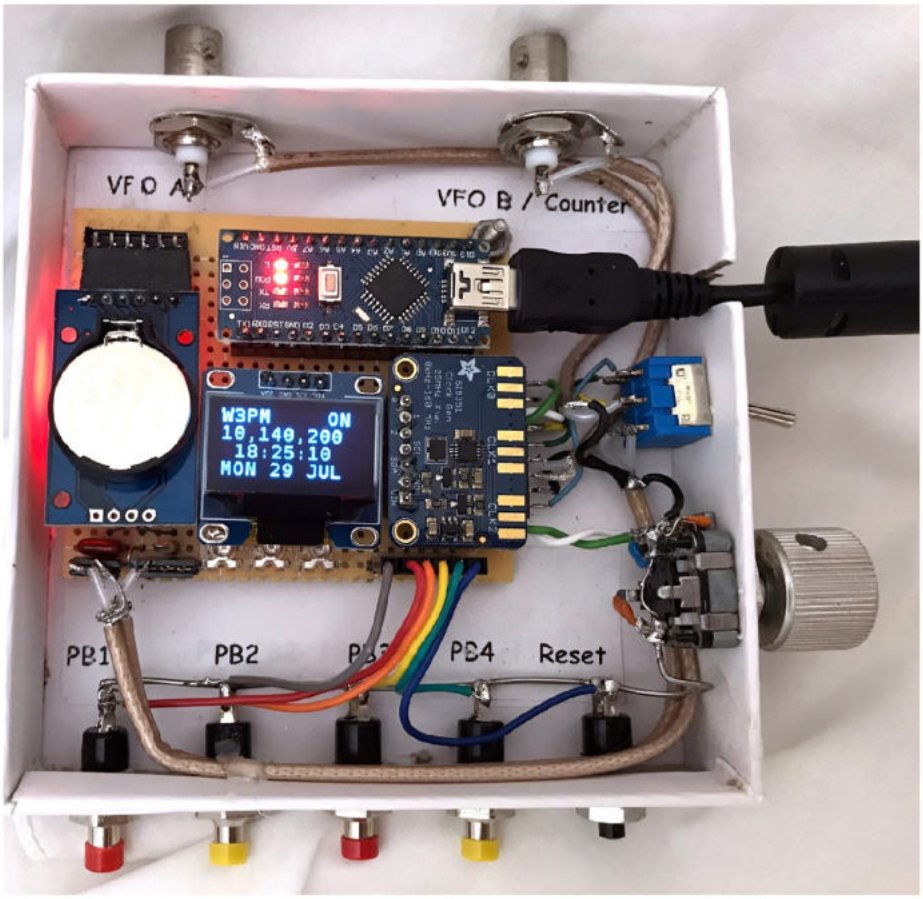

Figure 2 — The completed unit with the WSPR function selected and frequency set to 10,140,200 Hz in the 30 m band. A discarded box from an Apple TV purchase houses the project. The clear plastic cover was removed for this image.

Operation

When the unit is turned on, the auto-calibration algorithm begins to calculate the correction factor for the Si5351A 25 MHz clock. This takes 40 seconds to complete. The internal DS3231 temperature compensation algorithm concurrently calculates its correction factor every 64 seconds. The correction factors are continuously updated, therefore you might see small frequency jumps for the first few minutes until the unit stabilizes.

When the unit is turned on, the function selection menu is first displayed beginning with the WSPR function. Depress pushbutton 3 (**PB3**) to scroll through the other functions. Depress pushbutton 2 (**PB2**) to select the desired function.

Once selected, all functions are controlled by pushbuttons. An outline of pushbutton operation is shown in **Table 1**. Depress the **MENU** pushbutton to exit and return to the original function selection.

WSPR

The WSPR output is a square wave, therefore an external low-pass filter for the desired band of operation is required to meet FCC regulations for spurious emissions. The WSPR function is designed to be used as a WSPR source driving a small external amplifier and a low-pass filter. However, operation at the unit's 5 mW level using an external low-pass filter and a good antenna will result in a surprising number of WSPR spots from a large geographical area depending upon the band used and band conditions.

Prior to WSPR operation, ensure that your call sign, grid square locator, and power level have been loaded into the sketch. Be sure the clock setting is accurate to within about 1 second before transmitting WSPR. Select the desired band using **PB3**. Band switching is the only way to change the frequency while in WSPR mode. The specific WSPR frequency within the 200 Hz window of each band is determined by the user-configured variable "*TXoffset*" within the sketch. Use **PB2** to turn the transmitter ON or OFF. When the display is showing that the WSPR transmitter is ON a WSPR transmission will begin on an even minute after a few minutes of stabilization time, and then repeat based upon the "*TXinterval*" schedule set within the sketch.

WSPR frequency accuracy is dependent

Table 1 — Outline of pushbutton operation.

Pushbutton	*WSPR*	*VFO*	*Counter*	*Clock*	*Set Clock*	*Set Date*
PB1	N/A	Decrease Frequency	N/A	N/A	Time sync / Set Hour	Set Day
PB2	ON/OFF	Increase Frequency	N/A	N/A	Set Minute	Set Month
PB3	Band Select	Band Select	N/A	N/A	N/A	Set Year
PB4	N/A	Resolution Select	N/A	N/A	Hold to change time	Hold to change date

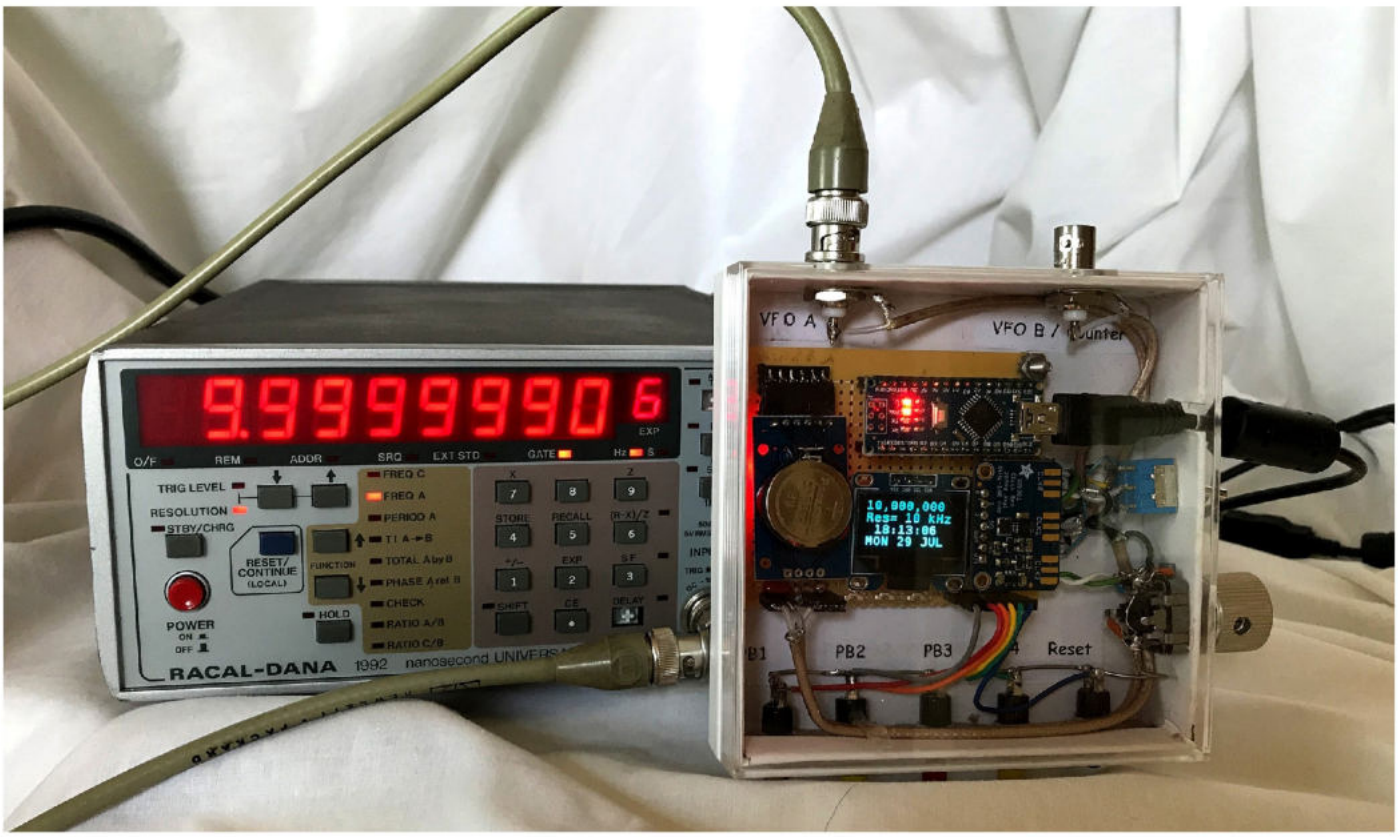

Figure 3 — The completed unit with the VFO function selected and set to 10 MHz using 10 kHz resolution.

upon the uncertainty of the DS3231 RTC, which is about 2 parts per million between 0 °C and 40 °C. This will keep transmissions within the 200 Hz WSPR window provided the sketch "*TXoffset*" is set to 1500 Hz, which is the middle of the WSPR window. If you want to use the optional in-band frequency hopping, or want to transmit nearer to the edge of the WSPR window, a calibration crystal aging offset register adjustment is documented near the end of the sketch.

Short term frequency stability during WSPR transmissions is particularly important on bands above 20 m. Short term drift stems from the Si5351 25-MHz oscillator and can be minimized by connecting a 50 Ω resistor or dummy load to the unused CLK2/VFO LO output during WSPR operation. Also, keep the unit enclosed and away from drafts.

VFO

The VFO frequency can be changed by using **PB3** to select the band and/or by using the pushbuttons **PB1** or **PB2** to decrease and increase the frequency. An optional rotary encoder can also be used. The resolution selection button (**PB4**) is used to change the frequency resolution in steps of 1 Hz, 10 Hz, 100 Hz, 1 kHz, 10 kHz, 100 kHz, and 1 MHz steps. Both the BFO and the LO outputs are available in addition to a CW offset. Instructions to implement these functions are documented within the sketch. The VFO output power is approximately 7 dBm (5 mW) depending upon the selected band. The frequency accuracy is dependent upon the uncertainty of the DS3231 RTC, which is about 2 ppm between 0 °C and 40 °C. The accuracy can be improved by adjusting the crystal aging offset of the DS3231 RTC. This is explained in the calibration documentation found near the end of the sketch.

Frequency Counter

After selecting the frequency counter function, change the position of the switch in Figure 1 to connect the output of the counter amplifier to pin D5 of the Arduino Nano. Be sure to return the switch to its normal position after using the frequency counter function.

The frequency counter is very basic with a bandwidth of approximately 6.5 MHz and an accuracy of about 3-4 ppm. The uncertainty is less than the VFO and WSPR because the unit uses a one-second gate time derived from the DS3231 RTC that is subject to some jitter. The gate time can be extended by changing the *gateTime* variable found in the sketch. A basic 2N2222 NPN transistor amplifier is used for the counter input. The input sensitivity is about -20 dBm throughout the frequency range. The maximum input voltage is about 5 V p-p.

Clock

The clock displays hour, minutes, seconds, and call sign. Every 10 seconds the display will alternate between the date (day of the week, date, and month) and temperature (°F and °C). The DS3231 measures its internal temperature, which will always be higher than the ambient temperature. A correction factor is used by the sketch to account for the difference, but do not expect the temperature readings to be very accurate.

Set Clock

Setting the correct time within ±1 second is critical for WSPR operation. The time is set by holding down **PB4** while depressing **PB1** to set hours or **PB2** to set minutes. At the top of the minute release **PB4**.

Provided the displayed time is correct to within ±30 seconds a shortcut to synchronize the time is available. Simply depress **PB1** at the top of the minute to synchronize the time.

(Continued on page 17)

Steve Franke, K9AN
3314 E. Anthony Dr., Urbana, IL 61802;
k9an@arrl.net

Bill Somerville, G4WJS
Glendella, Wycombe Rd., Stokenchurch,
High Wycombe HP14 3RP, England;
g4wjs@classdesign.com

Joe Taylor, K1JT
272 Hartley Ave., Princeton, NJ 08540;
k1jt@arrl.net

The FT4 and FT8 Communication Protocols

Motivation and design of the digital modes FT4 and FT8, and some details of how they are implemented in WSJT-X.

1. Introduction

FT4 and FT8 are digital protocols designed for rapid and accurate communication between amateur radio stations, particularly in weak-signal conditions. Information exchanged in a minimal two-station contact typically consists of call signs, four-character Maidenhead locators, signal reports, and acknowledgments. Special message formats support a few popular radio contests, and arbitrary text can also be conveyed, though only in small quantities. FT8 was introduced in July 2017 with version 1.8 of the software package *WSJT-X* **[1, 2]**. It quickly gained world-wide popularity, by some measures soon accounting for a large fraction of all ham radio activity on the high frequency (HF) bands **[3]**. FT4, a similar but faster protocol designed especially for radio contests, was introduced two years later in *WSJT-X* version 2.1.

The new protocols build on the legacies of JT4, JT9, JT65, and other digital modes pioneered in *WSJT-X* and its parent program *WSJT*, going back nearly 20 years **[4-11]**. These modes all use time-synchronized transmissions and structured messages with lossless compression of standard call signs, grid locators, and other basic information into a minimum number of bits. Strong forward error correction (FEC) is an integral part of each mode. FT8 and FT4 use a low density parity check (LDPC) block code designed and optimized specifically for this application.

Fundamental tenets of communication theory imply trade-offs involving message length, signaling rate, bandwidth, error-control coding, modulation type, decoding complexity, and minimum required signal-to-noise ratio (SNR). Earlier digital modes found in *WSJT-X*, including JT4, JT65, and QRA64, were optimized for extreme weak-signal performance on the VHF, UHF, and microwave bands. These modes use transmit and receive sequences of one minute, so two-way contacts generally require at least four minutes. By reducing the T/R sequences to just 15 seconds, optimizing the LDPC decoder in several important ways, and accepting a sensitivity loss (relative to JT65) around 4 dB, FT8 seems to have struck a sweet spot for DXing and general use on the HF, VHF, and lower UHF bands. FT4 accepts a further 3.2 dB loss in sensitivity but is twice as fast as FT8, and is potentially attractive for contesting at high QSO rates.

In this paper we provide full documentation of the FT4 and FT8 protocols and outline how the modes are implemented in *WSJT-X*. We present detailed performance measurements based on simulations over the additive white Gaussian noise (AWGN) channel and a range of standard International Telecommunications Union (ITU) models for HF propagation **[12]**. *WSJT-X* is an open source program licensed under version 3 of the Free Software Foundation's General Public License (GPLv3). We provide some guidelines and a few restrictions on the use of our freely available source code by others.

2. Structured Messages and Source Encoding

FT4 and FT8 transmissions always convey exactly 77 bits of user information. Mappings between human-readable messages and the underlying information bits depend on designed-for-the-purpose compression techniques known as *source encoding*. The basic aim is to give the 77-bit information payload maximum utility for conveying the information necessary for basic station-to-station contacts. To facilitate efficient message compression for a range of targeted purposes, we allocate three bits to specify one of eight possible message types. The remaining 74 bits are for user information, with source-encoding details that depend on message type. Types are tagged with an integer variable that we call `i3`, and types that require fewer than 74 information bits can use the remaining bits to define subtypes tagged as `i3.n3`.

Table 1 presents a summary of

Table 1 - Defined message types for the 77-bit payloads of FT4, FT8, and MSK144.

Type `i3.n3`	*Purpose*	*Example message*	*Bit-field tags*
0.0	Free Text	TNX BOB 73 GL	f71
0.1	DXpedition	K1ABC RR73; W9XYZ <KH1/KH7Z> -08	c28 c28 h10 r5
0.3	Field Day	K1ABC W9XYZ 6A WI	c28 c28 R1 n4 k3 S7
0.4	Field Day	W9XYZ K1ABC R 17B EMA	c28 c28 R1 n4 k3 S7
0.5	Telemetry	123456789ABCDEF012	t71
1.	Std Msg	K1ABC/R W9XYZ/R R EN37	c28 r1 c28 r1 R1 g15
2.	EU VHF	G4ABC/P PA9XYZ JO22	c28 p1 c28 p1 R1 g15
3.	RTTY RU	K1ABC W9XYZ 579 WI	t1 c28 c28 R1 r3 s13
4.	NonStd Call	<W9XYZ> PJ4/K1ABC RRR	h12 c58 h1 r2 c1
5.	EU VHF	<G4ABC> <PA9XYZ> R 570007 JO22DB	h12 h22 R1 r3 s11 g25

all currently defined message types. Each type has a defined human-readable format that is mapped into a sequence of fixed-length bit fields, each conveying specific information relevant to the type. Successive columns of **Table 1** show for each message type the number `i3` or `i3.n3`, the basic purpose, an example message, and a sequence of one or more bit-field tags. Numbers in the tag names indicate the number of bits in that field, and the total number of bits, including `n3` (if used) and `i3`, is always 77.

Table 2 identifies the type of human-readable information conveyed by each distinct bit-field tag. The tags include ones to encode call signs, Maidenhead locators, signal reports, acknowledgments, various logical flags, and permissible exchanges for a few special operating activities such as VHF contests, ARRL RTTY Roundup, and ARRL Field Day.

Standard amateur call signs can be conveyed in 28 bits, but compound calls such as PJ4/K1ABC and special-event calls like YW18FIFA may require more than twice that number. To accommodate such special calls, message type 4 allows use of one arbitrary call sign with up to 11 alphanumeric characters. The other call sign in such messages is sent as a *hash code* of just 12 bits. Such a mapping from call sign to hash code is uniquely defined, but obviously the inverse mapping cannot be unique. When the *WSJT-X* receiving software finds a message containing a hash code it displays the most recently decoded call sign mapping to that code (or perhaps "mycall", if it maps to that code), enclosed in angle brackets: for example `<PJ4/K1ABC>`. If no call sign is available for the received hash, the missing information is displayed to the user as `<...>`. Different message types may use different hash code lengths. For example, message type 0.1 always sends the transmitting station's call sign as a 10-bit hash code, and message type 1 conveys any call enclosed in angle brackets as a 22-bit hash code. Hash code "collisions" are possible, of course, but in practice we find they are rare. Further low-level details of these and other source encoding algorithms, including ranges of permitted values, can be found in Appendix A.

Table 2 - Assigned purposes for the bit fields listed in Table 1. Numbers in the tags indicate the number of bits in that field.

Tag	*Information conveyed*
c1	First callsign is CQ; h12 is ignored
c28	Standard callsign, CQ, DE, QRZ, or 22-bit hash
c58	Nonstandard callsign, up to 11 characters
f71	Free text, up to 13 characters
g15	4-character grid, Report, RRR, RR73, 73, or blank
g25	6-character grid
h1	Hashed callsign is the second callsign
h10	Hashed callsign, 10 bits
h12	Hashed callsign, 12 bits
h22	Hashed callsign, 22 bits
k3	Field Day Class: A, B, ... F
n4	Number of transmitters: 1-16, 17-32
p1	Callsign suffix /P
r1	Callsign suffix /R
r2	RRR, RR73, 73, or blank
r3	Report: 2-9, displayed as 529 – 599 or 52 - 59
R1	R
r5	Report: -30 to +32, even numbers only
s11	Serial number (0-2047)
s13	Serial Number (0-7999) or State/Province
S7	ARRL/RAC Section
t1	TU;
t71	Telemetry data, up to 18 hexadecimal digits

3. Error Detection and Error Correction

A 14-bit cyclic redundancy check (CRC) is appended to each 77-bit information packet to create a 91-bit message-plus-CRC word. The CRC is calculated on the source-encoded message, zero-extended from 77 to 82 bits. The CRC algorithm uses the polynomial 0x6757 (hexadecimal) and an initial value of zero (see **[13, 14]** for further details). Another 83 bits are appended for forward error correction, creating a 174-bit codeword.

Forward error correction is accomplished using a (174, 91) LDPC code designed specifically for FT8 and FT4. The code is defined by two matrices: a *generator matrix* used to compute the 83 parity bits appended to each 91-bit message-plus-CRC word, and a *parity matrix* that can be used to determine if a given 174-bit sequence is a valid codeword. All values in both matrices are either 0 or 1, and their related operations use modulo 2 binary arithmetic. The generator matrix has 83 rows and 91 columns. It is defined in a file `generator.dat` and included along with a number of other useful files in reference **[14]**. Nonzero values in row i of the matrix specify which of the 91 message-plus-CRC bits must be summed, modulo 2, to produce the i^{th} parity-check bit. Similarly, a file `parity.dat` **[14]** defines the sparse 83 × 174 parity-check matrix. The locations of the 1s in each row of this matrix specify which bits of a 174-bit codeword must sum (modulo 2) to zero. The 174-bit word is a valid codeword only if all 83 sums are zero.

4. Channel Symbols and Modulation

FT8 messages are transmitted using 8-tone continuous-phase frequency shift keying (CPFSK). Each transmitted tone or *channel symbol* conveys three bits. The sequence of 174 codeword bits is mapped onto a sequence of 174/3 = 58 channel symbols a_n, with n running from 0 to 57. The value of each symbol corresponds to a tone index in the range 0 to 7. Groups of three consecutive message bits are mapped to channel symbols using a Gray code defined by columns 1 and 2 of **Table 3**. This mapping ensures that bit triads associated with adjacent tones differ in only one bit position, thereby improving decoding performance on channels where Doppler spread is comparable to the tone separation.

FT4 is similar but uses 4-tone CPFSK, so each channel symbol conveys only two message bits. The sequence of 174 codeword bits is mapped onto a sequence of 174/2 = 87 channel symbols a_n, $n = 0$, 1, 2, ..., 86, with each symbol value an integer tone index in the range 0 – 3. Pairs of successive message bits are mapped to channel symbols according to the Gray code defined by columns 1 and 3 of **Table 3**.

Tone patterns known as *Costas arrays* are embedded in FT8 and FT4 waveforms to allow the receiving software to synchronize properly with received signals in both time and frequency. For FT8 we use the seven-tone sequence 3, 1, 4, 0, 6, 5, 2 inserted at the beginning, middle, and end of the transmitted waveform. If

Table 3 - Bi-directional Gray mapping between message bits and channel symbols.

Channel Symbol	*FT8 Bits*	*FT4 Bits*
0	000	00
1	001	01
2	011	11
3	010	10
4	110	
5	100	
6	101	
7	111	

the sync sequence is denoted S and the first and second halves of the information symbols by $M_A = \{a_0, a_1, ..., a_{28}\}$, and $M_B = \{a_{29}, a_{30}, ..., a_{57}\}$, the complete set of 79 transmitted symbols can be written as the sequence $b_n = \{S, M_A, S, M_B, S\}$.

Synchronization in FT4 uses four different Costas arrays, defined as follows:

$$S_1 = \{0,1,3,2\},$$
$$S_2 = \{1,0,2,3\},$$
$$S_3 = \{2,3,1,0\},$$
$$S_4 = \{3,2,0,1\}.$$

FT4 transmissions contain 87 information-carrying symbols. We divide these into three groups of 29:

$$M_A = \{a_0, a_1, ..., a_{28}\},$$
$$M_B = \{a_{29}, a_{30}, ..., a_{57}\},$$
$$M_C = \{a_{58}, a_{59}, ..., a_{86}\}.$$

To minimize keying transients we add a special ramp symbol R with tone index 0 that establishes slow transitions from zero amplitude at the start and to zero at the end of each waveform. A complete set of 105 channel symbols is then assembled as the sequence of values

$$b_n = \{R, S_1, M_A, S_2, M_B, S_3, M_C, S_4, R\}.$$

5. Generated Waveforms

Both protocols use continuous-phase frequency shift keying, which implies generated waveforms of the form

$$s(t) = A\cos\left(2\pi f_c t + \phi(t)\right).$$

Here A is signal amplitude, f_c is carrier frequency, t is time, and $\phi(t)$ is phase. The phase term can be written as the integral of instantaneous frequency deviation, $f_d(t)$,

$$\phi(t) = 2\pi\int_0^t f_d(\tau)\,d\tau, \quad t \geq 0.$$

This scheme guarantees that $\phi(t)$ is continuous, even across discontinuous steps in f_d. Signal amplitude A is constant, except for enforced rise and fall times at the start and end of a transmission. This constant-amplitude or *constant envelope* feature ensures that nonlinear amplification of the signal will not generate intermodulation products.

Frequency deviation $f_d(t)$ is evaluated as the weighted sum of a sequence of pulses, $p(t)$:

$$f_d(t) = h\sum_n b_n p(t - nT). \quad (1)$$

Here h is called the modulation index, weights b_n are the channel symbol values, $p(t)$ is the frequency deviation pulse shape, and T the signaling interval. (Note that T is the inverse of the keying rate, usually measured in bauds.) The frequency deviation pulse is normalized to have unit area,

$$\int_{-\infty}^{\infty} p(t)\,dt = 1, \quad (2)$$

so the pulse weighted by symbol b_n causes the carrier phase to advance by $2\pi h b_n$ radians over the duration of the pulse. For *WSJT-X* modes other than FT4 and FT8, $p(t)$ is a rectangular pulse with duration T and peak amplitude $1/T$. For these modes the instantaneous frequency deviation of the n^{th} pulse is hb_n/T.

The pulse amplitudes, b_n, are integers in the range 0 – 7 for FT8 and 0 – 3 for FT4. With this convention the carrier frequency f_c is the lowest tone frequency, i.e., the frequency transmitted during an interval with $b_n = 0$. The occupied bandwidth and spectral shape of the CPFSK signal depend on the modulation index, h, the signaling interval T, and the shape of the frequency deviation pulse $p(t)$. These parameters are summarized in **Table 4**, where for comparison we include, in addition to FT4 and FT8, several other modes supported in *WSJT-X*. The modes JT4, JT9, JT65, and MSK144 use rectangular frequency-deviation pulses, so their frequency deviations f_d have discontinuous jumps when b_n changes from one signaling interval to the next. Such jumps create relatively large spectral sidelobes in the CPFSK signal. In FT4 and FT8 the sidelobes are minimized by smoothing the frequency deviation function $f_d(t)$ with a Gaussian filter. Waveforms generated in this way are called Gaussian Frequency Shift Keyed (GFSK) signals.

Smoothing the frequency deviation waveform directly would require a numerical convolution every time a new message is generated. It is computationally more efficient to apply the Gaussian smoothing filter to an isolated rectangular pulse, which needs to be done only once. The Gaussian-smoothed pulses can then be superposed according to Equation (1) to obtain the GFSK frequency deviation waveform. Such waveforms are equivalent to those obtained by first generating the FSK waveform with rectangular pulses and then convolving it with a Gaussian smoothing function.

The GFSK Gaussian-smoothed pulse satisfying the normalization condition (2) can be written in terms of the error function, erf(x), as

$$p(t) = \frac{1}{2T}\left[\mathrm{erf}\left(kBT\left(\frac{t}{T} + 0.5\right)\right) - \mathrm{erf}\left(kBT\left(\frac{t}{T} - 0.5\right)\right)\right]. \quad (3)$$

Here the constant $k = \pi\sqrt{2/\ln 2} = 5.336...$, and B is the smoothing filter's -3 dB bandwidth. The error function erf(x) is defined as

$$\mathrm{erf}(x) = \frac{2}{\sqrt{\pi}}\int_0^x e^{-t^2}\,dt.$$

A Gaussian smoothing filter has a low-pass frequency response with Gaussian shape. For FT8 we set the -3 dB bandwidth to $B = 2T^{-1}$, or $BT = 2$. FT4 uses a more heavily smoothed pulse with

Table 4 - Parameters of the CPFSK signals used for six modes in *WSJT-X*. Pulse amplitudes assume integer values over the specified ranges.

Mode	*T(s)*	*Modulation index, h*	*Pulse shape, p(t)*	*Pulse amplitude, b_n*
FT4	0.048	1	Gaussian-smoothed, BT=1	0 – 3
FT8	0.160	1	Gaussian-smoothed, BT=2	0 – 7
JT4	0.2286	1	Rectangular	0 – 3
JT9	0.5760	1	Rectangular	0 – 8
JT65	0.3715	1	Rectangular	0, 2 – 65
MSK144	0.0005	0.5	Rectangular	0 – 1

$BT = 1$. In the limit of very large filter bandwidth, $BT \gg 1$, the pulse shape $p(t)$ defined by Equation (3) becomes rectangular and equivalent to the pulse used to generate standard FSK as in the older *WSJT* modes. The frequency deviation pulses actually used in *WSJT-X* are plotted for comparison in **Figure 1**.

Duration of the smoothed FT4 and FT8 pulses is greater than the signaling interval T, so successive pulses overlap. This intersymbol interference (ISI) is introduced deliberately for the purpose of shaping the emitted spectrum to reduce sidelobe levels. For the values of BT used in FT4 and FT8, significant ISI is present only between immediately adjacent pulses. Thus, when summing pulses to produce $f_d(t)$ using Equation (1), at time t it is only necessary to include contributions from the pulse whose center is closest to t and those immediately before and after it.

Figure 2 shows a portion of an FT4 frequency deviation waveform $f_d(t)$. It's easy to see that corners of the waveform at symbol boundaries have been rounded. As an example to illustrate the reduction in spectral sidelobes effected by using GFSK, **Figure 3** shows the spectrum of an FT4 signal and one generated using standard FSK with no smoothing. The difference in sidelobe levels is striking. The compact spectra of FT4 and FT8 signals make it possible for dozens of them to occupy a spectral slice of a few kHz, with little or no inter-signal interference.

FT4 and FT8 waveforms have constant amplitude except at the very beginning and end of a transmission. FT8 signals are ramped up gradually over a transition interval $T/8$, or 20 ms, at the beginning of the first sync symbol. The ramp function is a raised cosine,

$$A(t) = 0.5\left[1 - \cos(8\pi t / T)\right], \qquad 0 \le t \le T/8.$$

Figure 4 illustrates the FT8 ramp function and the leading part of an FT8 waveform. The same taper is used in reverse to gradually ramp down the signal at the end of the transmission. FT4 waveforms are similarly soft-keyed, this time using raised-cosine tapers applied over the full 48 ms duration of the special ramping symbols R, described earlier.

6. Symbol Detection and Decoding

Sections 2 through 5, Appendix A, and resources in reference **[14]** define the source encoding, error-correction coding, and modulation scheme associated with the FT4 and FT8 protocols. Any proper implementation of these protocols should strictly adhere to these definitions. In this section we turn to a discussion of some implementation-specific methods used in *WSJT-X* for detecting

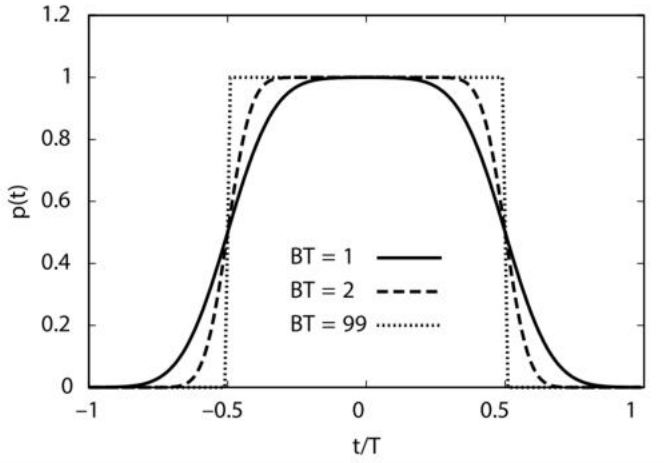

Figure 1 — Gaussian-smoothed frequency deviation pulses. The pulses labeled BT=1 and BT=2 are used to generate the FT4 and FT8 frequency-deviation waveforms, respectively. The case BT=99 is essentially the same as the unfiltered rectangular pulse that is used to generate standard, unsmoothed FSK in JT65, JT9, and other modes in *WSJT-X*.

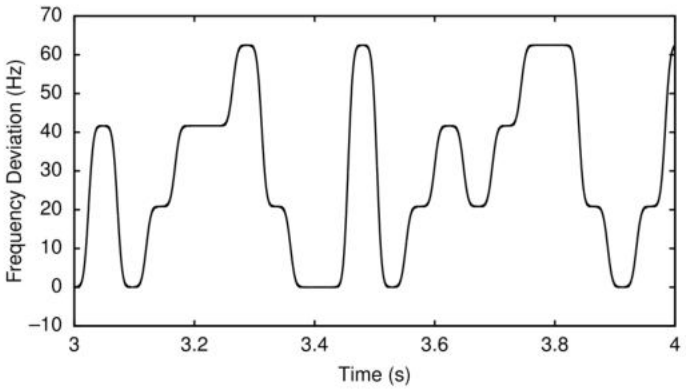

Figure 2 — A segment of an FT4 frequency deviation waveform generated using the Gaussian-smoothed frequency deviation pulse with BT=1.0.

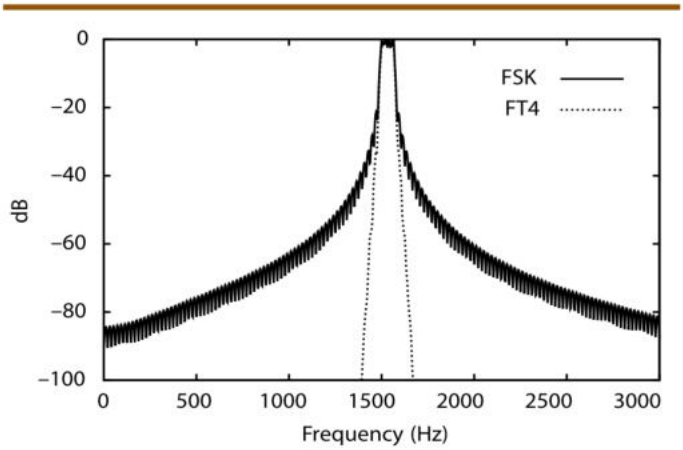

Figure 3 — Average spectrum of an FT4 signal (GFSK, BT=1.0: dotted line) and the spectrum of an otherwise equivalent standard FSK waveform (solid line).

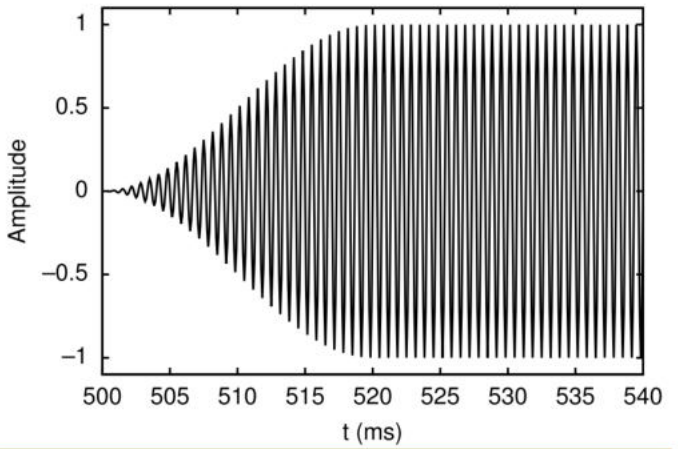

Figure 4 — The beginning of an FT8 waveform showing gradual rise of the signal envelope over the first 20 ms. FT4 uses a similar raised-cosine ramp expanded to 48 ms duration. Time-reversed ramp-down functions are used at the ends of transmissions.

and decoding FT4 and FT8 signals. Other approaches are certainly possible, and might be used by other software developers.

WSJT-X uses advanced detection and decoding techniques to decode the weakest possible signals. *Noncoherent block detection* over sequences of two or more channel symbols improves sensitivity over single-symbol detection when the received signal maintains phase coherence over multiple symbols **[15]**. Single-symbol detection provides robust detection on rapidly fading channels, while longer block lengths provide better sensitivity in slow fading conditions. We use block lengths of $N = 1$, 2, and 3 symbols for FT8, and $N = 1$, 2, and 4 for FT4.

Block detection is carried out by correlating received waveform segments spanning N symbols with locally generated waveforms corresponding to each of M^N possible symbol sequences. Here M is the number of different modulation waveforms (tones) used for each mode, $M = 8$ for FT8 and $M = 4$ for FT4. For this technique to provide sensitivity gains the received signal must be phase-stable over the block length. Such detection is said to be *noncoherent*, however, because phase continuity between sequences is not assumed. Only the magnitude of the complex-valued correlation is used, and detection is independent of phase differences between the received signal and locally generated waveforms. Output from the block detector is a set of M^N positive real correlation values. These are used to derive soft decisions for each of the $N \log_2 M$ bits conveyed by the N- symbol sequence.

Conversion of the waveform correlations to soft decisions is accomplished using a *soft demapper*. The soft metric L_j for x_j, the j^{th} bit associated with a particular symbol sequence, can be written as

$$L_j = K\left(\max_{i:x_j=1}|C_i| - \max_{i:x_j=0}|C_i|\right),$$

where $\max_{i:x_j=1}|C_i|$ is the largest correlation magnitude from the set of $M^N/2$ correlations between the received waveform and ideal waveforms associated with bit sequences having $x_j = 1$. Likewise, the second term is the largest magnitude from the other half of the set of correlations, associated with $x_j = 0$. The normalization constant, K, is adjusted empirically to optimize performance over a range of SNRs and channel conditions. For example, consider block detection of sequences of $N = 3$ successive FT8 symbols. Since each symbol could have any one of $M = 8$ values, there are $8^3 = 512$ possible three-symbol waveforms to be correlated with each three-symbol block of the received waveform. The resulting 512 correlation values determine soft decisions for the 9 bits conveyed by the sequence. In practice, *WSJT-X* calculates the 8 correlations required for single-symbol ($N = 1$) detection first, using a fast Fourier transform. The single-symbol complex results are then combined to produce the 64 correlations required for $N = 2$ and the 512 correlations required for $N = 3$ block detection, thereby avoiding needless redundant calculations.

A set of 174 soft decisions is obtained for each block size. These are submitted to the decoder, starting with the set for $N = 1$. If the decoder returns a codeword whose 77-bit message produces a 14-bit CRC that matches the decoded CRC, the algorithm terminates and the decoded message is unpacked and displayed to the user.

Our decoder uses a hybrid approach that combines the fast, iterative, *belief propagation* (BP) algorithm **[16]** with the more sensitive but computationally expensive *ordered statistics decoding* (OSD) algorithm **[16]**. In practice we find that most received signals are decoded with just a few iterations of the BP algorithm. When BP fails to find a valid codeword after a reasonable number of iterations, the soft decisions are submitted to the OSD algorithm. The OSD algorithm can provide several dB of additional sensitivity under certain conditions. Our implementation of the OSD algorithm incorporates the preprocessing rules from reference **[17]**. We found that these shortcuts significantly improve the computational efficiency of the OSD approach.

Our decoders can optionally make use of so-called *a priori* (AP) information as it accumulates during a QSO. For example, when you answer a CQ you already know your own call sign, that of your potential QSO partner, and the type of message you expect to receive if your reply is successful. Your decoding software therefore "knows" what might be expected for at least 62 message bits (29 for each of two call signs and /R flags, 1 for the R indicator, 3 for message type) in the next received message. With these bits hypothesized as a conjecture, the decoder's task can be reduced to determining the remaining 15 bits of the message and ensuring that the resulting solution is reliable. The use of AP information can increase sensitivity by several dB at the cost of a somewhat higher rate of false decodes.

Table 5 shows measured decoding thresholds for FT4 and FT8 derived from simulations, providing insight into the sensitivity gains offered by block detection and OSD. Here and elsewhere in this paper, quoted sensitivity thresholds are the signal-to-noise ratios in 2500 Hz bandwidth at which decoding probability is 0.5. Numbers in the first table row for each mode represent a baseline case with single-symbol $N = 1$ detection and BP decoding. The next two rows add block detection and block detection with hybrid (BP and OSD) decoding. Column 2 gives results for the non-fading additive white Gaussian noise (AWGN) channel, while columns 3 and 4 are for channels with frequency spreads of 1 Hz and 10 Hz, respectively. See Section 8 for more information about the channel models. One can see that on the AWGN channel block detection improves sensitivity by 1.6 dB and 0.7 dB for FT4 and FT8, respectively. Addition of hybrid decoding provides another 0.6 dB and 0.5 dB. Overall, block detection and the hybrid decoder offer 2.2 and 1.2 dB of sensitivity improvement over the baseline case for FT4 and FT8, respectively. On the mid-latitude disturbed channel, block detection improves sensitivity by 1.3 dB and 0.5 dB, and overall improvements are 2.5

Table 5 - Decoding thresholds for three different channels and three decoding schemes.

Decoding Algorithm	*AWGN (dB)*	*Mid-latitude Disturbed (dB)*	*High-Latitude Moderate (dB)*
FT4:			
N=1; BP	–15.3	–12.7	–10.4
N=1,2,4; BP	–16.9	–14.0	–10.5
N=1,2,4; BP+OSD	–17.5	–15.2	–12.2
FT8:			
N=1; BP	–19.6	–16.5	-
N=1,2,3; BP	–20.3	–17.0	-
N=1,2,3; BP+OSD	–20.8	–18.6	–8.6

and 2.1 dB. Doppler spread on the high-latitude disturbed channel exceeds the FT8 tone spacing, and FT8 fails to achieve a 50% decode probability at any SNR using only the baseline decoding scheme. With its larger tone spacing FT4 outperforms FT8 on this channel. Block detection does not offer significant improvement in this case — only 0.1 dB for FT4 — because coherence time on this rapidly fading channel is comparable to or smaller than the durations of the multi-symbol blocks.

After a signal is decoded we have the information necessary to regenerate the waveform that was actually transmitted. We use the regenerated signal as a reference to derive the time-varying, complex gain function that describes the effect of the propagation channel. Denote the real received audio signal by $s(t)$ and define a complex reference signal by

$$r(t) = A(t)e^{j(2\pi f_0 t + \phi(t))},$$

where f_0 is the estimated audio frequency of the decoded signal and $A(t)$ and $\phi(t)$ are the amplitude and phase of the transmitted waveform. The time-varying complex channel gain function, $g(t)$, is obtained via:

$$g(t) = LPF\left[s(t)r^*(t)\right],$$

where $LPF[\ ]$ represents a low-pass filter and * represents the complex conjugate. The low-pass filter cutoff is optimized for best performance with real signals received under a range of different propagation conditions. The estimated channel gain function is applied to the ideal reference signal to reconstruct a nearly noiseless version of the received signal's waveform, including channel-induced amplitude fading and phase variation. The reconstructed signal is then subtracted from the received data, i.e.

$$s'(t) = s(t) - 2\Re\left[g(t)r(t)\right]$$

where $\Re[\ ]$ takes the real part of its argument, and $s'(t)$ is the audio waveform after subtracting the decoded signal. This subtraction process can uncover weaker signals that occupy the same frequency slot as the subtracted strong signal. The weaker signals can often be decoded on a second decoding pass, after all signals decoded in the first pass have been subtracted.

WSJT-X analyzes an audio waveform that may contain many signals in the received passband. A decoding pass starts by identifying all likely signals, or *candidates*, using spectral analysis. Then, for each candidate in succession, our procedure is to (1) *synchronize*, estimating the frequency offset from the upper-sideband dial frequency and the time offset with respect to the computer's system clock; (2) determine soft decisions for each of three block lengths and attempt to decode each one using either BP alone or BP+OSD; (3) if the decode is successful, subtract the signal. If at least one signal is decoded and subtracted in the first decoding pass, the remaining audio waveform is re-analyzed. New candidates are identified and steps 1 through 3 are carried out for each one. If at least one new signal is decoded and subtracted in the second pass, a third pass will sometimes yield decodes missed in the first two passes. Multi-pass decoding has proven very effective: the approach is often able to decode two or three signals at the same or nearly the same frequency.

Acronyms and abbreviations used in text.

AP	*a priori*, as in AP decoding
AWGN	additive white Gaussian noise
BP	belief propagation
CPFSK	continuous-phase frequency-shift keying
CRC	cyclic redundancy check
FEC	forward error correction
GFSK	Gaussian frequency-shift keying
GPLv3	General Public License, version 3
ISI	inter-symbol interference
ITU	International Telecommunication Union
LDPC	low-density parity check code
MinGW	Minimalist GNU for Windows
OSD	ordered statistics decoding
SNR	signal-to-noise ratio
UI	user interface

7. Message Sequencing

A basic QSO between K1JT and K9AN might consist of the following messages:

```
Tx6: CQ K1JT FN20
                        Tx1: K1JT K9AN EN50
Tx2: K9AN K1JT -10
                        Tx3: K1JT K9AN R-12
Tx4: K9AN K1JT RRR
                        Tx5: K1JT K9AN 73
```

Here the Txn: labels are those used to identify message entry fields on the *WSJT-X* user interface. In this model QSO even-numbered messages are sent by K1JT, odd-numbered messages (those displaced to the right) by K9AN. Note that all messages bear the transmitting station's call sign, and all but the CQ are explicitly directed to a particular QSO partner. Most QSOs follow the sequence shown, or a closely related one depending on context, propagation, and interference conditions. In normal usage, failure to decode a response from a QSO partner implies repetition of the previous transmission.

Traditionally, operators have clicked buttons on the user interface (UI) of *WSJT-X* **[1, 2, 19]** and its predecessor *WSJT* **[4-11]** to trigger transmission of the next message in a sequence similar to that shown above. Protocols with one-minute T/R sequences leave about 10 seconds between decoding and start of the next transmission, so there is plenty of time to decide upon and activate one's next transmission. However, the shorter sequences of FT8 and FT4 require much quicker responses, effectively requiring moderate amounts of automation built into the software.

If a UI checkbox labeled **Auto Seq** has been ticked, the software parses decoded messages to decide whether a valid response for the standard QSO sequence has been received, directed to "mycall". If so, the next message in the sequence is queued and transmitted; if not, the previous transmission is repeated. This sequence of events proceeds until a QSO is completed or abandoned by user action. With a few optional exceptions ("Fox" operation in FT8 DXpedition mode, and contest operation), user action is also required to verify QSO details and submit them for logging. In any event, by design *WSJT-X* requires that every QSO must be initiated by a human operator. We do not like the idea of fully robotic operation with modes like FT4 and FT8, and the *WSJT-X* software prevents it.

These moderate levels of automation involve considerably more logic in the software, essentially duplicating the thought processes of an attentive user progressing through a valid QSO. In typical operation on a busy HF or VHF band, dozens of valid FT4 or FT8 messages may be decoded in a single receiving sequence. The receiving software must analyze all of these, determine whether any is a valid reply in the expected sequence for a QSO already underway, and take appropriate action. **Figure 5** provides a high-level summary of the six major states of the *WSJT-X* auto-sequencing behavior. On program startup, and when **Halt Tx** is clicked, the logical *state machine* is put into the Calling state. Subsequent stages of a standard

QSO pass through the Replying, Report, Roger_Report, Rogers, and Signoff states while proceeding through the sequence of transmitted and received messages illustrated at the start of this section.

Each major state has its own internal logic that determines what action will be taken when specified types of messages are received. An idealized and abbreviated representation of this logic for the Calling state is presented in **Figure 6**. Here and in **Figure 5** we have used Unified Modeling Language notation **[18]**, which should be mostly self-explanatory. For example, the text

[message == Tx1] / Tx message = Tx2

attached to a state transition line has the form "trigger [guard condition] / action," so this is a transition that happens automatically without any triggering event, but only if the just parsed message has the standard Tx1 format. In this case the transition has a side effect of setting the next message queued for transmission as the generated Tx2 message.

The user interface provides options for configuring various details of the auto-sequencing behavior; please consult the *WSJT-X 2.1 User Guide* **[19]** for further details.

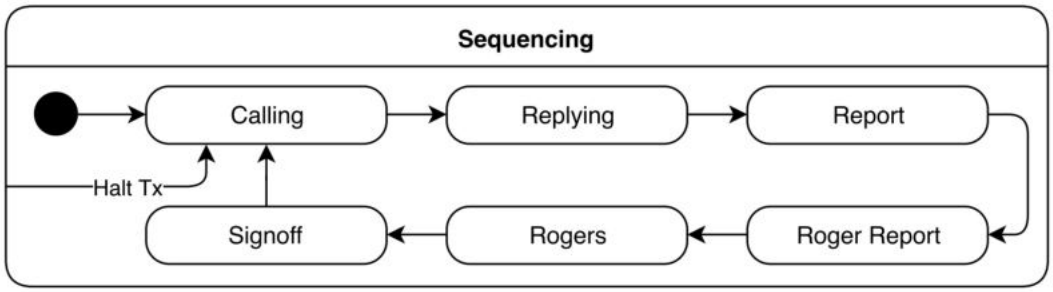

Figure 5 — Top-level state diagram for standard message sequencing in WSJT-X.

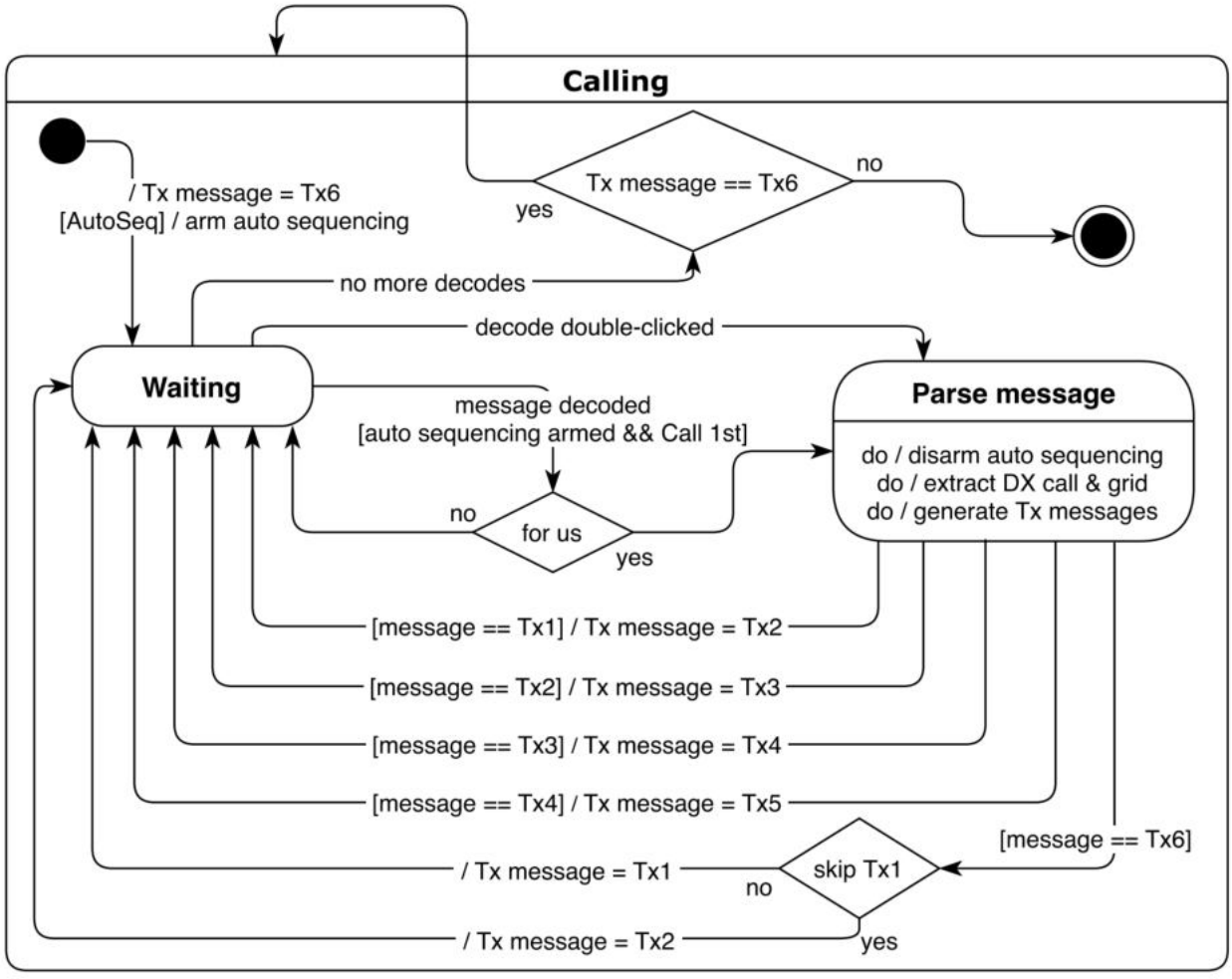

Figure 6 — Example detailed state chart for the high-level "Calling" state shown in Figure 5.

8. Performance Measurements

While designing FT4 and FT8 we used channel simulations based on the approach recommended by the ITU **[12]** to assess the performance that could be achieved under real-world conditions. The channel model assumes two independently fading paths with equal mean attenuation and equal frequency spreads. A channel is defined by its frequency spread and differential path delay. Reference **[12]** specifies frequency spread and path delay parameters for quiet, moderately disturbed, and highly disturbed conditions in low-latitude, mid-latitude, and high-latitude terrestrial regions. The ITU channels referenced in this paper have differential path delays that are small compared to FT4 and FT8 symbol durations, so this parameter has little effect on performance. The size of a channel's frequency spread relative to the tone spacing of the mode is the most important factor determining the extent of performance degradation.

Figure 7 compares FT4 and FT8 performance obtained using *WSJT-X* version 2.1 to decode simulated FT4 and FT8 waveforms under non-fading additive white noise (AWGN) conditions, and on *mid-latitude disturbed* and *high-latitude moderately disturbed* channels. **Table 6** lists the channel parameters and the decoding threshold for these channels along with the *mid-latitude quiet* and *mid-latitude moderate* channels. FT8 maintains about 3 dB sensitivity advantage over FT4 on AWGN and mid-latitude channels where frequency spread is smaller than the tone spacing for both modes. Frequency spread on the high-latitude channel is larger than the FT8 tone spacing and smaller than FT4's tone spacing, which explains why FT4 performs best in that case.

Table 6 includes decoding thresholds obtained when the maximum possible amount of AP information is available. Maximum AP information provides about 2 dB of additional sensitivity on less disturbed channels and increasing improvement as frequency spread increases. On the most disturbed channel, large improvements of about 5 dB and 10 dB are obtained for FT4 and FT8, respectively. The trend is similar for scenarios where less AP information is available.

Figure 8 provides a detailed look at how using AP information can improve sensitivity as a QSO progresses. The *mid-latitude disturbed* channel was used for this set of simulations. The curve labeled "no AP" is the same as the curve labeled "FT8 Mid disturbed" **Figure 7**. The curve labeled "caller" shows sensitivity to responses to a CQ, or any other message directed to "mycall". The curve labeled "report" indicates sensitivity to messages directed to "mycall", originating from the known call sign of a QSO partner. This curve represents the sensitivity to a report or roger-report message during a QSO. Finally, the curve labeled "RRR/RR73/73" represents sensitivity to an RRR, RR73, or 73 message from a QSO partner, at the end of a QSO.

Figure 8 shows a modest sensitivity improvement to a caller when only "mycall" is used as AP information. The advantages of such AP information become more significant when the caller fails to start transmitting at the nominal start time, 0.5 s after the

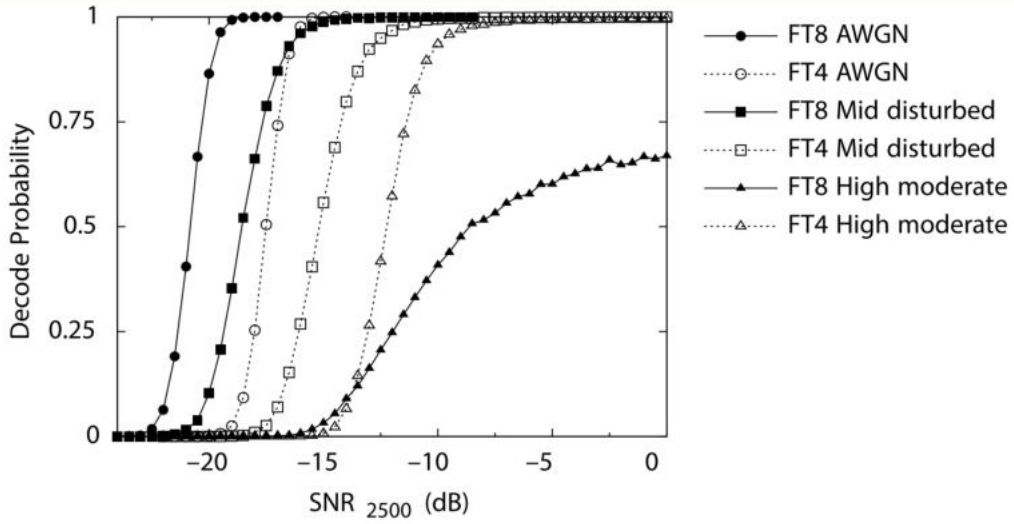

Figure 7 — Measured decoding probability as a function of SNR for FT8 and FT4, based on simulations for three propagation channels: additive white Gaussian noise (AWGN), and the ITU standards for mid-latitude disturbed and high-latitude moderate conditions. No AP information was used for these sensitivity measurements.

Table 6 - FT4 and FT8 decoding thresholds measured using simulations. In all cases, the decoder used block detection and (BP+OSD). For each channel and mode, two decoding thresholds are given. "No AP" is the threshold when no a priori information is available, and "max. AP" is the decoding threshold with the maximum amount of a priori information, at the end of a QSO when receiving RRR, 73, or RR73 from a QSO partner.

Channel	*Frequency Spread (Hz)*	*Diff. Path Delay (ms)*	*FT4 Decoding Threshold (dB), no AP*	*FT4 Decoding Threshold (dB), max. AP*	*FT8 Decoding Threshold (dB), no AP*	*FT8 Decoding Threshold (dB), max. AP*
AWGN	0.0	0.0	–17.5	–19.5	–20.8	–22.7
Mid-latitude quiet	0.1	0.5	–17.4	–19.4	–20.0	–22.4
Mid-latitude moderate	0.5	1.0	–15.8	–18.6	–18.8	–22.1
Mid-latitude disturbed	1.0	2.0	–15.2	–18.4	–18.6	–22.1
High-latitude moderate	10.0	3.0	–12.2	–17.4	–8.6	–18.9

beginning of a transmit interval. In such cases, *WSJT-X* will skip the missed part of the transmission and start sending a correctly synchronized message for the remainder. Those receiving such a truncated message will collect only a fraction of the message symbols. A common scenario for this occurrence is "late" responses to a CQ. For example, suppose that G4WJS calls CQ. He knows that responses to his call will be addressed to G4WJS. The "no AP" curve in **Figure 9** shows that without the use of AP information, responses from callers who start transmitting more than 5 seconds after the beginning of a Tx interval will not be decoded. The curve labeled "AP mycall" shows decoding probability as a function of start time when the decoder specifically looks for responses directed to G4WJS. In this case transmissions that were started up to 8 seconds late are likely to be decoded successfully.

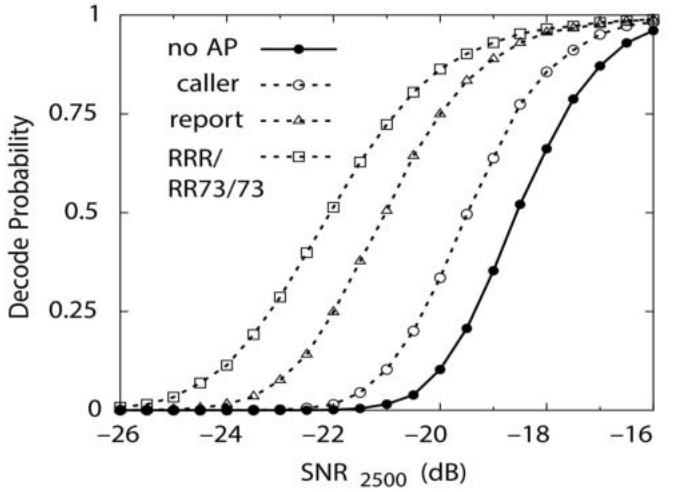

Figure 8 — Decode probability for FT8 on the mid-latitude disturbed channel using different amounts of a priori (AP) information. See text for details.

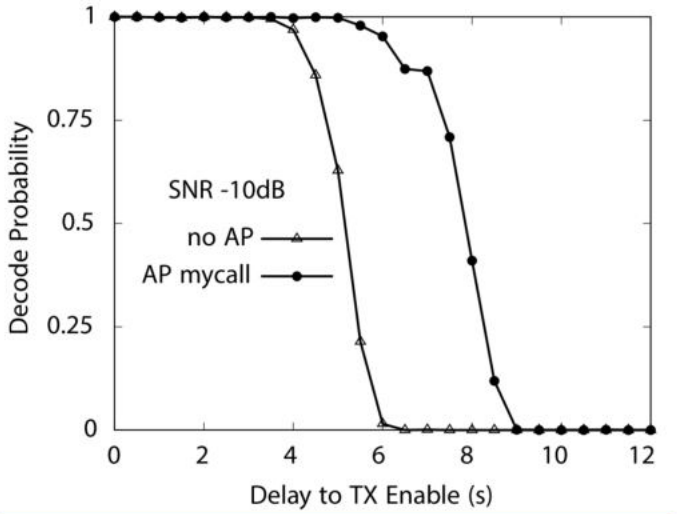

Figure 9 — Decode probability for FT8 when the transmitting station starts transmitting after the beginning of a 15 s interval. The simulation was performed for the mid-latitude moderately disturbed channel, at SNR = –10 dB. The kink in the "AP mycall" curve at 6.5 s arises because missing symbols from the Costas array in the middle of the FT8 transmission have little effect on decoding probability.

9. Concluding Remarks and Software License

This paper and the online resources found in reference **[14]** provide complete descriptions of the FT4 and FT8 protocols. In the spirit of open sharing, and to encourage other software developers who might use some of our ideas, we place this description in the public domain with the following restrictions:

- Other software implementers may use the names "FT4" and "FT8" only if they adhere to our protocol definitions for source encoding, error-correction coding, and modulation format.
- Robotic or unattended QSOs must be explicitly disallowed.
- *Multi-streaming* with waveforms and message content similar to those used in FT8 DXpedition Mode is permissible only within the guidelines specified in the *WSJT-X 2.1 User Guide* **[19]**.
- Presently unassigned message types (see **Table 1**) are reserved for future expansion and must not be assigned without our permission.
- Any implementation of these or similar protocols that allows robotic, unattended, or non-conforming multi-streaming operation shall not use the names "FT4" or "FT8" and must be made incompatible by some means, such as using different Costas arrays for synchronization.

With the exception of code contained in reference **[14]**, source code for our implementations of FT4, FT8, and MSK144 is *not* in the public domain. Rather, all code in *WSJT-X* is copyrighted and licensed under the terms of Version 3 of the GNU General Public License (GPLv3), reference **[20]**. Very briefly stated, GPLv3 guarantees end users the freedom to run, study, and modify the software, so long as the same licensing terms are extended to any new software derived from or dependent upon our source code.

We welcome any independent software implementations of FT4 and FT8, so long as they either (1) adhere to all requirements mentioned above, or (2) make no use of our source code beyond the public-domain resources mentioned above. We hope and trust that many of the innovations pioneered in *WSJT-X* and its predecessors will outlive its present developers — and will continue to advance the art of weak-signal communication by Amateur Radio for many years to come.

Appendix A. Source Encoding Details

Section 2 of this paper is a summary of how the FT4, FT8, and MSK144 protocols pioneered in *WSJT-X* compress and convey call signs, Maidenhead locators, signal reports, and certain other information in a very efficient way. **Tables 1 and 2** outline the basic source-encoding framework, with each message payload comprising a sequence of fixed-length bit fields. This Appendix completes the details needed to fully define mappings from human-readable message fragments to relevant fields in the fixed-size 77-bit message payload. For the convenience of others who might wish to implement the FT4 or FT8 protocols, some essential algorithmic parts of the definitions are presented in simple, very short Fortran programs whose source code we have placed in the public domain **[14]**.

As first steps we shall define the way standard call signs and 4-character Maidenhead locators are encoded into fields of just 28 and 15 bits, respectively. As described in the *WSJT-X 2.1 User Guide* **[19]**, a standard amateur call sign consists of a one- or two-character prefix, at least one of which must be a letter, followed by a decimal digit and a suffix of up to three letters. Within these rules, the number of possible call signs is equal to 37×36×10×27×27×27 =

262,177,560. (The numbers 27 and 37 arise because in the first and last three positions a character may be absent, or a letter, or perhaps a digit.) Since 2^{28} = 268,435,456 is a larger number, 28 bits are enough to encode any standard call sign uniquely, while leaving 6,257,896 values available for conveying other types of information. A few of these excess values are assigned to special message components such as DE, QRZ, and CQ (optionally with a modifier). A further 2^{22} = 4,194,304 are used to convey 22-bit hash codes for call signs.

Similarly, there are 180×180 = 32,400 four-digit Maidenhead grid locators. This number is less than 2^{15} = 32,768, so a grid locator can be uniquely represented in 15 bits. Some of the 368 fifteen-bit values not needed for grid locators are used to convey numerical signal reports of the form ±*nn* in the range -30 to +99 dB, or a blank, or one of the words RRR, RR73, or 73.

As a particular example, consider the bit allocations for message type 1, an essential part of almost all FT4 and FT8 QSOs. These basic messages usually contain two 28-bit call signs, an optional acknowledgment R, and a four-character locator, signal report, RRR, RR73, or 73. **Table 1** shows that this message type consists of fields with the tags `c28`, `r1`, `c28`, `r1`, `R1`, `g15`, and `i3`. The `r1` fields are normally 0; the value 1 implies a /R call sign suffix to indicate "rover" status in a North American VHF contest. The `R1` field conveys the absence (0) or presence (1) of an acknowledgment R before the locator or signal report conveyed by `g15`. In the final 77-bit information payload, bit fields are assembled in the left-to-right order specified in **Table 1**, followed by `n3` (if used; currently used only in type 0) and `i3`.

We now turn to concise descriptions of the algorithms mapping human-readable message fragments to the tagged bit fields with names listed in **Table 2**. For this purpose the public-domain Fortran programs contained in reference **[14]** are essential. To get started, download the compressed tarfile `ft4_ft8_protocols.tgz` from the **www.arrl.org/QEXfiles** web page, unpack it into a suitable directory and follow simple instructions for your operating system (Windows, Linux, or macOS) at the top of file `Makefile`. These steps will build executables for the seven programs `gen_crc14`, `free_text_to_f71`, `grid4_to_g15`, `grid6_to_g25`, `hashcodes`, `nonstd_to_c58`, and `std_call_to_c28` whose purposes are explained below.

In alphabetical order, concise definitions for the tagged bit fields listed in **Table 2** are as follows:

`c1:` Used only in message type 4. Normally 0; value 1 denotes a message consisting of CQ and a nonstandard call sign, for example `CQ PJ4/K1ABC`.

`c28:` Used to convey a standard call sign or one of the special message words CQ, DE, or QRZ, or a 22-bit call sign hash code. CQ may be followed by a modifier with three decimal digits or one to four letters. Each possible message fragment with CQ, DE, or QRZ is mapped to a specific integer value of `c28`, as indicated in **Table 7**. Call sign values are computed using the algorithm illustrated by program `std_call_to_c28`, and hash codes by program `hashcodes`.

`c58:` Used to encode nonstandard call signs up to 11 characters, using the algorithm illustrated by program `nonstd_to_c58`.

`f71:` Conveys arbitrary free text with up to 13 characters selected from the list `0123456789ABCDEFGHIJKLMNOPQRSTUVWXYZ+-./?` plus the blank character. The encoding algorithm is illustrated by program `free_text_to_f71`.

`g15:` Encodes a 4-character Maidenhead locator, signal report, RRR, RR73, 73, or a blank message word, using the algorithm in program `grid4_to_g15`.

`g25:` Encodes a 6-character Maidenhead locator using the algorithm in program `grid6_to_g25`.

`h10, h12, h22:` Call sign hash codes of length 10, 12, or 22 bits. The hashing algorithm is defined in program `hashcodes`.

`k3:` ARRL Field Day Class A-F, encoded as integer values 0 – 5.

`n4:` In message type 0.3, maximum number of simultaneously transmitted signals minus 1. In message type 0.4, maximum number of simultaneously transmitted signals minus 17.

`p1:` Absence (0) or presence (1) of call sign suffix /P.

`r1:` Absence (0) or presence (1) of call sign suffix /R.

`r2:` Value 0 encodes a blank message word; values 1 – 3 encode RRR, RR73, or 73.

`r3:` Values 0 – 7 encode a signal report displayed as 52, 53, … 59 (message type 0.3) or 529, 539, … 599 (type 3).

`R1:` Absence (0) or presence (1) of acknowledgment R before grid or report.

`r5:` Values 0 – 31 convey signal reports –30, –28, … +32 dB (even numbers only).

`s11:` Serial number, range 0 – 2047.

`s13:` Values 0 – 7999 convey a serial number; values 8001 – 8065 encode the abbreviations for US states and Canadian provinces by means of lookup table `states_provinces.txt` included in reference **[14]**.

`S7:` Values 0 – 83 encode abbreviations for the ARRL/RAC section names by means of lookup table `arrl_rac_sections.txt` included in reference **[14]**.

`t1:` Absence (0) or presence (1) of TU; at the start of a type 3 message.

`t71:` Telemetry data, up to 18 hexadecimal digits or 71 bits maximum. With 18 digits, the first digit must fall in the range 0 – 7.

We note here that for FT4 only, in order to avoid transmitting a long string of zeros when sending CQ messages, the assembled 77-bit message is bitwise exclusive-OR'ed with the following pseudo-random sequence before computing the CRC and FEC parity bits:

```
01001010010111110100010
01101101001011000010000
10100111100101010101110
11111000101
```

The receiving software applies this exclusive-OR procedure a second time, to restore the original 77-bit message.

Table 7 - Summary of mappings between message fragments and numerical values of the bit field *c28*.

Message fragment	*c28 as decimal integer*
DE	0
QRZ	1
CQ	2
CQ 000 - CQ 999	3 to 1002
CQ A - CQ Z	1004 to 1029
CQ AA - CQ ZZ	1031 to 1731
CQ AAA - CQ ZZZ	1760 to 20685
CQ AAAA - CQ ZZZZ	21443 to 532443
22-bit hash codes	2063592 + (0 to 4194303)
Standard call signs	6257896 + (0 to 268435455)

Steve Franke, K9AN, holds an Amateur Extra class license. He was first licensed in 1971 and has previously held call signs WN9IIQ and WB9IIQ. An early and abiding fascination with radio science led to a 35-year career as Professor of Electrical and Computer Engineering at the University of Illinois. Steve retired in 2019 and now holds the title Professor Emeritus. He enjoys chasing DX, playing with RF circuits and antennas, and studying HF and VHF propagation. Steve is a member of ARRL and a Fellow of the IEEE.

Bill Somerville, G4WJS, earned a Chemistry degree at the University of Bristol and has worked in computer software and hardware in a variety of industries including defense, software development, and financial services. Most recently he's a freelance consultant providing systems programming and related services to mid- to large-size software tool vendors. An active radio amateur since 1981, Bill enjoys HF and VHF bands, contest operating, and DX chasing using CW, phone, and data modes.

Joe Taylor was first licensed as KN2ITP in 1954, and has since held call signs K2ITP, WA1LXQ, W1HFV, VK2BJX and K1JT. He was Professor of Astronomy at the University of Massachusetts from 1969 to 1981 and since then Professor of Physics at Princeton University, serving there also as Dean of the Faculty for six years. He was awarded the Nobel Prize in Physics in 1993 for discovery of the first orbiting pulsar, leading to observations that established the existence of gravitational waves. After retirement he has been busy developing and enhancing digital protocols for weak-signal communication by Amateur Radio, including JT65 and WSPR. He chases DX from 160 meters through the microwave bands.

References

[1] Joe Taylor, K1JT, Steve Franke, K9AN, and Bill Somerville, G4WJS, "Work the World with *WSJT-X*: Part 1, Operating Capabilities," *QST*, Oct. 2017, pp. 30-36.
[2] Joe Taylor, K1JT, Steve Franke, K9AN, and Bill Somerville, G4WJS, "Work the World with *WSJT-X*: Part 2, Codes, Modes, and Cooperative Software Development," *QST*, Nov. 2017, pp. 34-39.
[3] "Mode Usage Evaluation: 2017 was 'the Year When Digital Modes Changed Forever'," **www.arrl.org/news/mode-usage-evaluation-2017-was-the-year-when-digital-modes-changed-forever**.
[4] Joe Taylor, K1JT, "WSJT: New Software for VHF Meteor-Scatter Communication," *QST*, Dec. 2001, pp. 36-41.
[5] Joe Taylor, K1JT, "EME with JT65," *QST*, June 2005, pp. 80–82.
[6] Joe Taylor, K1JT, "The JT65 Communications Protocol," *QEX*, Sep./Oct. 2005, p. 3-12.
[7] Rex Moncur, VK7MO, and Joe Taylor, K1JT, "Small Station EME at 10 and 24 GHz: GPS Locking, Doppler Correction, and JT4," *Dubus* 2/2013.
[8] Steven J. Franke, K9AN, and Joseph H. Taylor, K1JT, "Open Source Soft-Decision Decoder for the JT65 (63,12) Reed-Solomon Code," *QEX*, May/June 2016, pp. 8-17.
[9] Steven J. Franke, K9AN, and Joseph H. Taylor, K1JT, "The MSK144 Protocol for Meteor-Scatter Communication," *QEX*, July/Aug. 2017, pp. 8-14.
[10] Nico Palermo, IV3NWV, "Q-ary Repeat-Accumulate Codes for Weak Signals Communications," **www.eme2016.org/wp-content/uploads/2016/08/EME-2016-IV3NWV-Presentation.pdf**.
[11] Joe Taylor, K1JT, "*WSJT-X*: New Codes, Modes and Tools for Weak-Signal Communication," **www.physics.princeton.edu/pulsar/K1JT/K1JT_EME_2016_Venice.pdf**.
[12] Testing of HF Modems with Bandwidths of up to about 12 kHz Using Ionospheric Channel Simulators, *Recommendation ITU-R F.1487*, International Telecommunications Union, 2000.
[13] Ross N. Williams, "A Painless Guide to CRC Error Detection Algorithms," **https://www.zlib.net/crc_v3.txt**.
[14] **http://physics.princeton.edu/pulsar/k1jt/ft4_ft8_protocols.tgz**.
[15] Marvin K. Simon and Dariush Divsalar, "Maximum-Likelihood Block Detection of Noncoherent Continuous Phase Modulation," *IEEE Transactions on Communications*, Vol. 41, No. 1, Jan. 1993, pp. 90-98.
[16] Shu Lin and Daniel J. Costello, Jr., **Error Control Coding: Fundamentals and Applications, 2nd edition**. Pearson Prentice Hall, 2004.
[17] Yingquan Wu and Christoforos N. Hadjicostis, "Soft-Decision Decoding of Linear Block Codes Using Preprocessing and Diversification," *IEEE Transactions on Information Theory*, Vol. 53, No. 1, Jan. 2007, pp. 378-393.
[18] **https://en.wikipedia.org/wiki/UML_state_machine**.
[19] WSJT Development Group, "WSJT-X 2.1 User Guide," **www.physics.princeton.edu/pulsar/K1JT/wsjtx-doc/wsjtx-main-2.1.2.html**.
[20] GNU General Public License, GPLv3, **https://www.gnu.org/licenses/gpl-3.0.txt**. See also **https://en.wikipedia.org/wiki/GNU_General_Public_License**.

Simple and Inexpensive Auto-Calibrating Multifunction Project

(Continued from page 6)

Set Date

The date is set by holding down **PB4** while depressing **PB1** to set the date, **PB2** to set the month, or **PB3** to set the year. Release **PB4** to save the changes.

DS3231 Aging Offset Adjustment

While the default RTC is already very accurate, its accuracy can be pushed even higher by adjusting its aging offset register. The documentation located at the end of the sketch provides methods to determine the correction factor and upload it to the aging offset register.

Figure 3 shows the unit set to 10 MHz and connected to a frequency counter after the aging offset was adjusted. For normal operation this adjustment is not required. The default 2 ppm accuracy of the RTC will result in an uncertainty of less than ±30 Hz on 20 meters.

If WSPR is used, the time will require synchronization every 7 to 10 days without offset adjustment. The re-synchronization time frame can be stretched to a month or more with proper adjustment.

Experimentation

This is an open source project. You are invited to experiment and improve upon system operation. Relatively simple system improvements can be made. For example, you can substitute a 1 pps output from a GPS unit for the 1 pps output from the DS3231 RTC board to further increase frequency (but not clock) accuracy.

Acknowledgement

I wish to thank Ronald Taylor, WA7GIL, for his suggestions to improve this project.

[Photos by the author.]

Gene Marcus, W3PM, GM4YRE, was first licensed in 1963 as KN3YVP and has held an Amateur Extra class license since 1968. He was first licensed in Scotland as GM5AQM in 1969 and received a First Class FCC Radiotelephone license in 1977. Gene completed the ASEE degree program at Penn State University in 1968. After a four-year tour as a Cryptologic Technician with the US Navy, he began a 32 year career in the field of precision measurement equipment calibration. In retirement Gene enjoys experimenting with various RF and microprocessor projects as well as world-wide travel with his wife Phyllis.

Eric P. Nichols, KL7AJ

3763 Lyle Ave., North Pole, AK 99705; **eric@alaskit.co**

The Versatile Double Balanced Mixer – Part 2

Something old, something new.

One of our alert *QEX* readers, Paul Gavrilovic of Allen, Texas wrote to the Editor and me regarding the double balanced mixer (DBM), in part:

Regarding historical references to the double balanced or ring mixer, there is a detailed summary paper in the April, 1939 edition of the Bell System Technical Journal *by R.S. Carruthers which describes DBM use in AT&T's carrier telephone systems. The mixers were made with copper oxide disks and were commercially deployed by 1939. The paper points out that "At least as early as 1927, copper oxide rectifiers were being tried as modulators for speech channels of carrier telephone systems in this country. … Since 1931 continued improvements in copper oxide rectifiers have rapidly increased their field of application until now they are employed in practically all modulators of the latest types of carrier telephone systems." I hope this will be interesting to* QEX *readers. — Paul Gavrilovic*

Likewise, I also hope this will be interesting to *QEX* readers. Thank you, Paul! We modern "techie" people can always benefit from a periodic reminder that we aren't as clever as we think we are. One of the nice things about having a substantial personal electronics library, one in which most of the tomes are older than *I* am, is that we can gain a wonderful new perspective on older technologies, or at least *presumed* older technologies. Perusing all this great literature has also given me something productive to do while riding out our corona virus siege. I was able to locate the very core of the text to which our alert reader refers: the November 1938 AT&T edition of "Principles of Electricity applied to Telephone and Telegraph Work," which

$$I = \frac{A \sin Vt}{2(R_1 + R_2)} + \frac{2A}{\pi(R_1 + R_2)} [\sin Vt \sin Ct + \tfrac{1}{3} \sin Vt \sin 3Ct + \tfrac{1}{5} \sin Vt \sin 5Ct + \cdots] \quad (165)$$

Here R_1 and R_2 are respectively the input and output resistances as indicated in Figure 356 and C is 2π times the carrier frequency.

Making use of the trigonometric relationship—

$$\sin\theta \sin\phi = \tfrac{1}{2}\cos(\theta - \phi) - \tfrac{1}{2}\cos(\theta + \phi),$$

the above equation may be rewritten as—

$$I = \frac{A \sin Vt}{2(R_1 + R_2)} + \frac{A}{\pi(R_1 + R_2)} [\cos(C - V)t - \cos(C + V)t + \tfrac{1}{3}\cos(3C - V)t - \tfrac{1}{3}\cos(3C + V)t + \tfrac{1}{5}\cos(5C - V)t - \tfrac{1}{5}\cos(5C + V)t + \cdots] \quad (166)$$

The first term of this equation represents the original signal voltage with a reduced amplitude. The first two terms inside the brackets are the lower and upper side-bands of the modulated carrier wave, and the remaining terms in the brackets represent similar upper and lower side-bands of odd multiples of the carrier frequency. The equation does not include any term for the carrier frequency itself, showing that the carrier is suppressed by the balanced arrangement of the varistors.

In practice, as we know, only one of the side-bands of the carrier frequency is made use of and this is selected from the several frequency terms appearing in the output by means of a suitable band-pass filter. A demodulator arrangement, identical to that shown in Figure 356, is used at the receiving end of the carrier line to restore the original signal frequency. In this case, the frequencies applied to the varistor circuit (demodulator) are the received side-band and a locally generated carrier identical in frequency to that supplied to the modulator at the sending end. Thus, if we assume that the lower side-band is transmitted, the signal frequency applied to the demodulator may be indicated in the form, $K\cos(C-V)t$. When this term is substituted in Equation (165) in place of $A \sin Vt$, the first term inside the brackets in Equation (166) will become:

$$\cos[C - (C - V)]t = \cos Vt$$

This is the desired original signal and it can be selected from the other components of demodulation by the use of a simple low-pass filter.

For the group modulators and demodulators of the Types-J and K carrier systems, a somewhat different arrangement of the varistor units is employed. This is illustrated in Figure 359. It is also a balanced bridge arrangement but the circuit connections and the configuration of the varistors are such that, as indicated in Figure 360, the signal voltage is impressed across the output transformer in one direction during one-half of the carrier cycle, and in the other direction during the other half of the carrier cycle. In other words the circuit acts like a reversing switch operating at the carrier frequency and results, in the ideal case, in the output current wave shown in Figure 361.

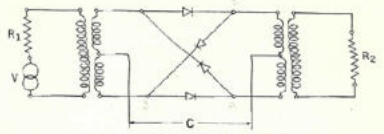

FIG. 359. LATTICE MODULATOR CIRCUIT

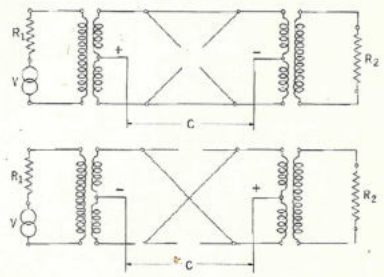

FIG. 360. OPERATING PRINCIPLE OF CIRCUIT OF FIG. 359

Using the same terminology as in the preceding discussion, the approximate equation for the curve of Figure 361 is—

$$I = \frac{2A}{\pi(R_1 + R_2)} [\cos(C - V)t - \cos(C + V)t + \tfrac{1}{3}\cos(3C - V)t - \tfrac{1}{3}\cos(3C + V)t + \tfrac{1}{5}\cos(5C - V)t - \tfrac{1}{5}\cos(5C + V)t + \cdots] \quad (167)$$

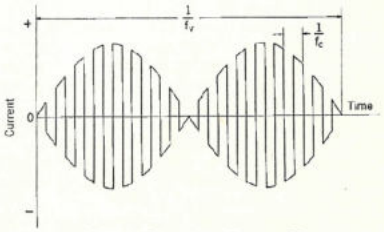

FIG. 361. OUTPUT CURRENT OF LATTICE MODULATOR

[259]

Figure 1 — Source: November 1938 AT&T edition of "Principles of Electricity applied to Telephone and Telegraph Work" page 259.

was for many years the *de facto* training text of AT&T employees. Scans of these pages are shown in **Figures 1** and **2**.

It really is amazing what some of our communications ancestors were able to do with some very primitive hardware, not the least of which were sub-par semiconductors. In 1938, the copper oxide rectifier was still the best thing they had available. But despite the fundamental component limitations, the circuit topology and concepts, many of which were developed by the telephone company, were astoundingly advanced. In fact, network theory hasn't come up with anything really new in the past 80 years or so.

What's particularly interesting is that closed-circuit *Single Sideband Suppressed Carrier* was already fairly well developed for long-distance telephone use by the late 1930s; it took another couple of decades for radio amateurs to fully catch on. And, of course, the versatile DBM was instrumental in this happening. However, in defense of our fellow radio amateurs, we have to concede that AT&T was far better funded than the average pre-WW2 ham to develop things like SSB. On the other hand, it's more than likely that a great number of those well-heeled AT&T engineers were hams, too.

Striking up the Baseband

One of the driving forces for advancing telephone technology was conserving copper. A wide variety of multiplexing methods were developed to pack more conversations onto a pair of copper wires, or even a single copper wire. If you think the ham bands are crowded on a contest weekend, think of all those hundreds of thousands, or millions, of talkers making long distance calls over twisted pairs of copper wires! Carrier current methods went a long ways toward increasing the number of available channels for a given TCC (Total Copper Content).

Now, while most of us radio amateurs are primarily concerned with *on-the-air* communications, many of us are revisiting the *baseband* characteristics of our signals. That is, what is happening to our signals, both analog and digital, *before* they are applied to a modulator and transmitter for radiation through the ether.

The double balanced mixer, or even more profoundly, a pair of *I* and *Q* double balanced mixers, allows untold manipulation of baseband signals. If you have a copy of *Fldigi* software on your shack computer, just look at all the modes available. All of these are generated with double balanced mixers, or at least digital software facsimiles of these devices. A DBM doesn't have to be made of silicon diodes, or even copper oxide rectifiers, but can be fully implemented in software. Remember that a balanced mixer is a *multiplier* circuit, and any mathematical function that can be done with analog devices can also be done with digital calculations. Not that it's always more *practical* to do things this way, but it is always possible in theory. For the most part, however, the "real" DBM is going to be around for a long time.

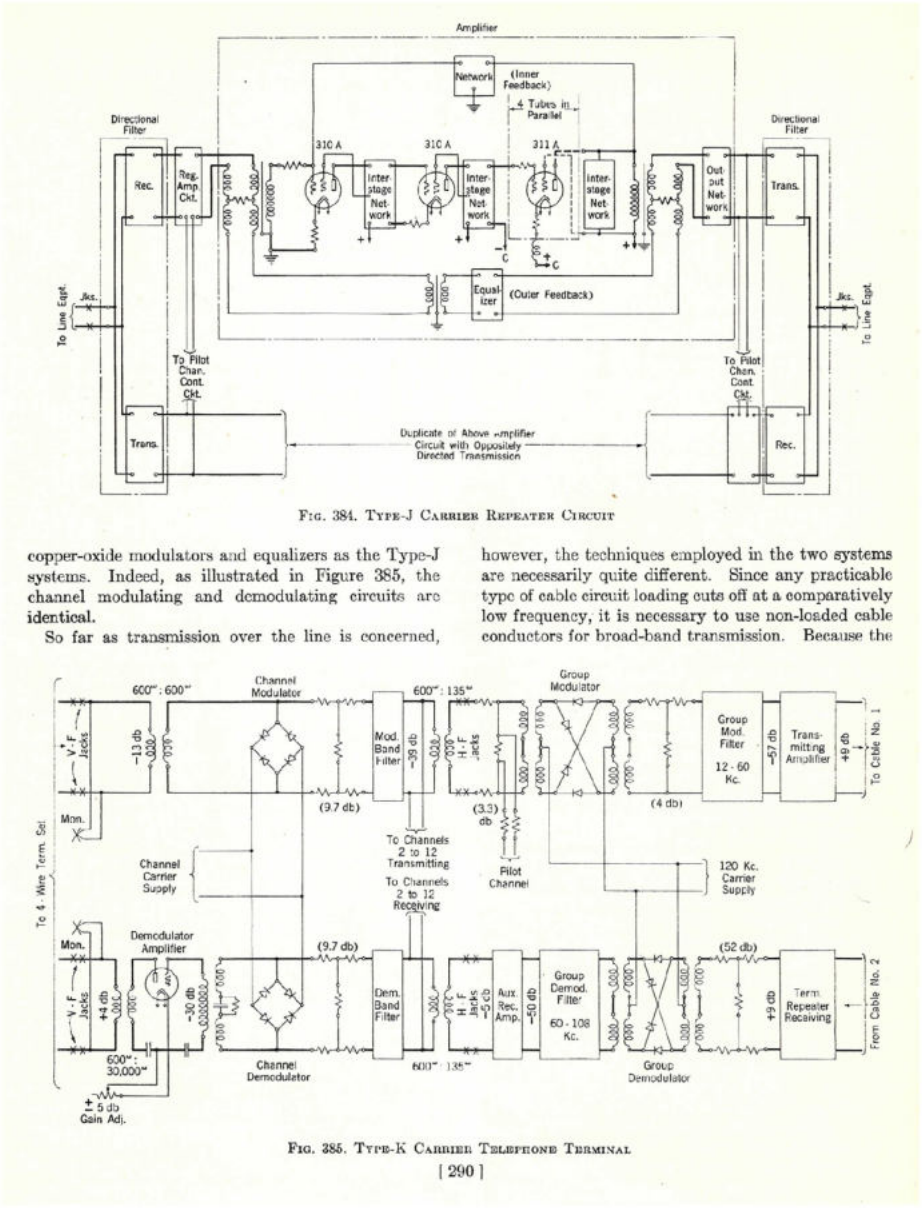

FIG. 384. TYPE-J CARRIER REPEATER CIRCUIT

copper-oxide modulators and equalizers as the Type-J systems. Indeed, as illustrated in Figure 385, the channel modulating and demodulating circuits are identical.

So far as transmission over the line is concerned, however, the techniques employed in the two systems are necessarily quite different. Since any practicable type of cable circuit loading cuts off at a comparatively low frequency, it is necessary to use non-loaded cable conductors for broad-band transmission. Because the

FIG. 385. TYPE-K CARRIER TELEPHONE TERMINAL

[290]

QX2007-Nichols02

Figure 2 — Source: November 1938 AT&T edition of "Principles of Electricity applied to Telephone and Telegraph Work" page 290.

Going through a Phase

Many, or most, of us "properly-seasoned" hams remember when the phasing-type SSB transmitter was the most practical means of generating a single sideband signal. The *pièce de résistance* in my ham shack is my beloved Central Electronics 100V shown in **Figure 3**. Not only can it generate upper and lower sideband, but it can also generate double sideband full carrier, double sideband suppressed carrier, upper sideband with carrier, lower sideband with carrier, and with AM, PM, CW, and FSK thrown in for good measure. Because the 100V has two double balanced mixers in quadrature, all implemented with vacuum tubes, it can create all these different modes with ease.

Figure 3 — The Central Electronics 100V transmitter uses two double balanced mixers in quadrature to generate a wide range of modulations.

So, as you can see, the whole idea of using *I/Q* modulation to generate a plethora of new modes, is anything but new. The 100V was manufactured between 1959 and 1960.

Now, one of the most difficult challenges of the phasing method was coming up with a 90° audio phase shifter. The 90° RF phase shift on the other hand was a trivial matter. But designing a network of any kind with a 90° phase shift over a 10:1 frequency range was, and still is, a real challenge. This is one task that digital signal processing (DSP) greatly simplified, and because of this, the phasing method is being "re-implemented" in most modern SSB transceivers and receivers.

Well, I hope this waltz through memory lane has been more than a pleasant distraction; we can learn a lot from our elder statesmen of radio.

In our next installment, we will explore in depth the phase detection principles of the DBM, and look at some unusual applications for this versatile building block.

Eric P. Nichols, KL7AJ, is a two-time recipient of the William Orr, W6SAI, Technical Writing Award. He has written numerous articles for QST *and* QEX *magazine as well as four ARRL books, the latest being "Receiving Antennas for the Radio Amateur." Eric's latest focus is on encouraging experimentation on our two new bands on 2200 meters and 630 meters, heroically attempting to make up for lost time in catching up with our LF brethren across the pond.*

Letters

A Simple Inexpensive Accurate Vector Impedance Meter, (Jan./Feb. 2020)

Dear Editor,

A few weeks ago I finished construction of three vector impedance meters described by Jim Koehler, VE5FP, in January/February 2020 *QEX*. I have one instrument and two ham colleagues have the others. The unit is a joy to work with and it produces excellent results. I commend Jim, VE5FP, and his colleague Thomas Alldread, VA7TA, for their excellent work.

The designers connected the two female BNC connectors directly to the case cover and soldered the circuit board on the opposite side. We opted to use a separate piece of aluminum and milled square holes in the cover for the BNC flanges (**Figure A**). This arrangement would let us remove the board as a complete assembly without unsoldering the connectors.

Soldering the SMT components wasn't difficult. I used flux on all contacts. For resistors and capacitors I put a small amount of solder on one pad, aligned the component and pressed down on it with my thumbnail. Next I heated the soldered pad and thumb pressure pushed the component into place. Then I soldered the other contact. Stay well. — *Jon Titus, KZ1G, Herriman, UT.*

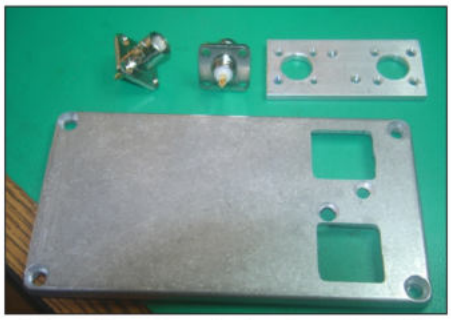

Figure A — Mounting hardware for BNC flanges.

The Versatile Double Balanced Mixer, (Mar./Apr. 2020)

Dear Editor,

I enjoyed reading the article "The Versatile Double Balanced Mixer" by E. Nichols, KL7AJ, in the March/April 2020 issue of *QEX*. Mr. Nichols' description of operating the DBM with dc applied to the IF port, thus unbalancing the circuit, was mostly new for me, although I was familiar with the phase detector configuration.

Regarding historical references to the double balanced or ring mixer, there is a detailed summary paper in the April, 1939 edition of the *Bell System Technical Journal* by R. S. Caruthers, which describes DBM use in the AT&T carrier telephone systems. The mixers were made with copper oxide disks and were commercially deployed by 1939. The paper points out that:

"At least as early as 1927, copper oxide rectifiers were being tried as modulators for speech channels of carrier telephone systems in this country. … Since 1931 continued improvements in copper oxide rectifiers have rapidly increased their field of application until now they are employed in practically all modulators of the latest types of carrier telephone systems."

I hope this will be interesting to *QEX* readers. — *Best regards, Paul Gavrilovic, Allen, TX.*

The author responds,

Hi Paul! This is actually quite humorous, because I happen to have a copy of that very tome of which you speak in my hand right now! I was debating whether to mention that piece in my article when I wrote it. I guess you have made the decision for me. I'll copy that page and insert it into my next installment. Great catch! — *73, Eric Nichols, KL7AJ, North Pole, AK.*

Send your *QEX* Letters to the Editor to, ARRL, 225 Main St., Newington, CT 06111, or by fax at 860-594-0259, or via e-mail to qex@arrl.org. We reserve the right to edit your letter for clarity, and to fit in the available page space. "Letters to the Editor" may also appear in other ARRL media. The publishers of *QEX* assume no responsibilities for statements made by correspondents.

Steve Stearns, K6OIK

P.O. Box 4917, Mountain View, CA 94040-0917; **k6oik@arrl.net**

Crest Factor of Sinusoidal Electromagnetic Fields

The author explores the relationship between peak instantaneous and rms values of EM fields.

We know from Amateur Radio license exams that for sinusoidal voltages and currents the ratio of peak-to-rms value is the square root of two. This ratio is ingrained into our intuitions about sinusoidal waveforms, whether they be voltages, currents, or anything else. The ratio of peak instantaneous to rms value of a periodic waveform is called its "crest factor," **[1]**. Crest factor is an important parameter in the design of amplifiers and communication modulations. Amplifiers must accommodate a modulation's crest factor without distortion. Hence amplifier designs strive to accommodate high crest factor, while modulation designs strive for low crest factor.

In electromagnetic field theory, we deal with electric fields and magnetic fields that are "vector" fields because they assign a vector value to every point in space at every instant of time. Radio is based on sending electromagnetic waves through space. The waves are undulations of the electric and magnetic fields that fill space. Waves travel. Fields do not travel, they merely occupy space. Fields are unique to an observer. Two observers in relative motion will generally see different fields, but the fields seen by each are related to those seen by the other. We save that story for another time.

If one sends a sinusoidal signal as a radio wave, the electric field vector's components are sinusoids, which at every point in space have a magnitude and phase. A basic question to ask is, what is the ratio of the peak instantaneous to rms value of the magnitude of the electric field? We seek an answer that is true for sinusoidal fields in general and not just for a propagating wave. Now this question seems simple. After all, if the fields are sinusoidal, isn't the ratio of peak to rms simply the square root of two? The surprising answer is no.

Sinusoidal, time-harmonic electric and magnetic fields may be described in the time domain or in the frequency domain. In both cases the fields are vectors. In the time domain the vector components are three real numbers that depend on location in space and time. In the frequency domain the vector components are the Fourier transforms of the time domain components. In the single-frequency sinusoidal case, the vector components are complex phasors, familiar to electrical engineers from *ac* circuit analysis. This paper explores the relationship between peak instantaneous and rms values when the field representation is given in terms of component phasors.

Phasors

A phasor is a way of representing a sine wave when there is only one frequency present. Instead of writing a sinusoidal voltage as

$$V(t) = A\cos\left(\omega t + \phi\right) \tag{1}$$

where $\omega = 2\pi f$ is frequency in radians per second, we use complex numbers to express (1) in the shorthand phasor notation,

$$\underline{V} = A\angle\phi = Ae^{j\phi} \tag{2}$$

The quantity $\underline{V}$ is called a phasor. Underbars are sometimes used to denote phasors. $\underline{V}$ is the complex amplitude of the voltage at time $t = 0$. The frequency $\omega = 2\pi f$ is understood. In the right side of (2), the phasor is written in Euler form as a complex exponential, where j is the unit imaginary, i.e. the square root of -1. The notations in (2) are familiar to electrical engineers from *ac* circuit theory. The notation was introduced and popularized by Charles Proteus Steinmetz at General Electric in the late 19th and early 20th centuries. Phasors are useful in the steady-state, single-frequency analysis of linear circuits and systems.

Representation of a sinusoidal field as a triplet of phasors

Sinusoidal field vectors can be represented in terms of complex vectors that have phasor components. A sinusoidal field may be expressed as a triplet of complex phasors, one phasor for each field component, **[2, pp. 15-16]**.

$$\begin{aligned}\mathbf{E}_\omega &= \underline{E}_x\,\mathbf{i} + \underline{E}_y\,\mathbf{j} + \underline{E}_z\,\mathbf{k} \\ &= \left(E_x\angle\phi_x\right)\mathbf{i} + \left(E_y\angle\phi_y\right)\mathbf{j} + \left(E_z\angle\phi_z\right)\mathbf{k} \\ &= \left(E_x e^{j\phi_x}\right)\mathbf{i} + \left(E_y e^{j\phi_y}\right)\mathbf{j} + \left(E_z e^{j\phi_z}\right)\mathbf{k}\end{aligned} \tag{3}$$

Each field component is a sinusoid having a peak value given by the magnitude of its respective phasor, that is, E_x, E_y, or E_z.

Representation of a sinusoidal field as a bivector

Another representation for sinusoidal fields is obtained by separating the real and imaginary parts of (3) into a sum of two vectors as follows.

$$\begin{aligned}\mathbf{E}_\omega &= \left(E_x e^{j\phi_x}\right)\mathbf{i} + \left(E_y e^{j\phi_y}\right)\mathbf{j} + \left(E_z e^{j\phi_z}\right)\mathbf{k} \\ &= \left[E_x \cos\phi_x \mathbf{i} + E_y \cos\phi_y \mathbf{j} + E_z \cos\phi_z \mathbf{k}\right] \\ &\quad + j\left[E_x \sin\phi_x \mathbf{i} + E_y \sin\phi_y \mathbf{j} + E_z \sin\phi_z \mathbf{k}\right]\end{aligned} \tag{4}$$

This gives two vectors that point in different directions unless the phase angles are equal. The two vectors are formally represented as a bivector or a 3×2 matrix. Six numbers are required to specify a sinusoidal field at a point in space. This number may be reduced in special cases. For example if the field represents a TE wave, and the field components are expressed in a coordinate system that aligns with the direction of wave travel, then one field component is zero. This apparent simplification comes at the expense of having to store three angles to represent a coordinate transformation. The bivector representation is presented in books on electrodynamics but is not useful for the problem of crest factor addressed here.

Instantaneous Peak and RMS Values Defined

A field **E** (or **H**) at a location (x, y, z) is a vector function of time. The magnitude of the field, denoted $|\mathbf{E}|$, is a scalar function of time. Peak and rms values are defined as the maximum and root-mean-square of $|\mathbf{E}|$ over a prescribed interval of time. In the sinusoidal case, the interval is one cycle or a time period of $T = 1/f = 2\pi/\omega$.

$$\begin{aligned}E_{Peak} &= \max_{0<t<T}\left\{\left|\mathbf{E}(t)\right|\right\} \\ E_{rms} &= \sqrt{\frac{1}{T}\int_0^T \left|\mathbf{E}(t)\right|^2 dt}\end{aligned} \tag{5}$$

The definitions in (5) do not depend on the vector's direction, nor do they require the direction to be constant during a cycle.

Root-mean-square (rms) of Field Magnitude

We will determine the peak instantaneous and rms field values defined in (5) from the field components specified in (3). The first step is to convert the component phasors in (3) into time domain notation to get the field vector

$$\begin{aligned}\mathbf{E}(t) &= E_x \cos(\phi_x + \omega t)\mathbf{i} \\ &\quad + E_y \cos(\phi_y + \omega t)\mathbf{j} \\ &\quad + E_z \cos(\phi_z + \omega t)\mathbf{k}\end{aligned} \tag{6}$$

The squared instantaneous magnitude of $\mathbf{E}(t)$ is

$$\begin{aligned}\left|\mathbf{E}(t)\right|^2 &= E_x^2 \cos^2(\phi_x + \omega t) \\ &\quad + E_y^2 \cos^2(\phi_y + \omega t) \\ &\quad + E_z^2 \cos^2(\phi_z + \omega t)\end{aligned} \tag{7a}$$

$$\begin{aligned}\left|\mathbf{E}(t)\right|^2 &= E_x^2 \frac{1+\cos\left(2(\phi_x + \omega t)\right)}{2} \\ &\quad + E_y^2 \frac{1+\cos\left(2(\phi_y + \omega t)\right)}{2} \\ &\quad + E_z^2 \frac{1+\cos\left(2(\phi_z + \omega t)\right)}{2}\end{aligned} \tag{7b}$$

$$\begin{aligned}\left|\mathbf{E}(t)\right|^2 &= \frac{1}{2}\left(E_x^2 + E_y^2 + E_z^2\right) \\ &\quad + \frac{1}{2}\begin{pmatrix} E_x^2 \cos(2\phi_x + 2\omega t) \\ + E_y^2 \cos(2\phi_y + 2\omega t) \\ + E_z^2 \cos(2\phi_z + 2\omega t)\end{pmatrix}\end{aligned} \tag{7c}$$

The first term is a constant independent of time. The second term is periodic at twice the fundamental frequency. Substituting (7) into the root-mean-square formula of (5), the harmonic term integrates to zero. Consequently the rms value of the field magnitude is given by the simple formula

$$\begin{aligned}E_{rms} &= \sqrt{\frac{1}{T}\int_0^T \left|\mathbf{E}(t)\right|^2 dt} \\ &= \frac{1}{\sqrt{2}}\sqrt{E_x^2 + E_y^2 + E_z^2}\end{aligned} . \tag{8}$$

Complex Vector Norms

Norms are commonly used in mathematics to measure the "size" or "magnitude" of mathematical entities such as numbers, vectors, matrices, and functions. Two norms that are relevant are the Lebesgue ℓ_2 vector norm and the Frobenius matrix norm.

The Lebesgue ℓ_2 norm of a vector is defined as

$$\left|\mathbf{E}\right|_{\ell_2} = \sqrt{\sum_{i=1}^{3}\left|e_i\right|^2} \tag{9}$$

The vertical bars on the left denote the norm, whereas the vertical bars in the summation represent either absolute value or complex magnitude according as the elements of the vector are real or complex numbers. In the case of a vector (3) whose components are phasors, we have

$$\begin{aligned}\left|\mathbf{E}_\omega\right|_{\ell_2} &= \sqrt{E_x^2 + E_y^2 + E_z^2} \\ &= \sqrt{2}E_{rms}\end{aligned} \tag{10}$$

from (8). The norm is the square root of the inner product of the vector with its conjugate vector. The result is called a Hermitian inner product. This idea can be extended to include vectors that are represented as column matrices by defining "inner product" as a Hermitian transposed row vector times a column vector, written as

$$\left|\mathbf{E}\right|_{\ell_2} = \sqrt{\mathbf{E}^H\mathbf{E}} \ . \tag{11}$$

The Frobenius norm applies to matrices. When a vector is represented as a column matrix, the Frobenius norm simplifies to the square root of the trace of a vector outer product matrix

$$\begin{aligned}\left\|\mathbf{E}\right\|_F &= \sqrt{\mathrm{Trace}\left[\mathbf{E}\mathbf{E}^H\right]} \\ &= \sqrt{\sum_{i=1}^{3}\left|e_i\right|^2}\end{aligned} . \tag{12}$$

The result is the same as the Lebesgue ℓ_2 norm or Hermitian inner product.

Such vector norm formulas, when applied to vector components specified as phasors, properly give energy or power averaged over a cycle but do not directly provide information about instantaneous values during a cycle. Hence the formulas applied directly to phasor components can determine root-mean-square but not peak instantaneous field magnitude during a cycle.

However norm formulas can be applied to time waveforms by treating waveforms as points in a function space. In this case the summations are replaced by integrals. If the time waveform is the instantaneous magnitude of the field vector, or $|\mathbf{E}(t)|$, two Lebesgue norms, the ℓ_∞ and ℓ_2 norms of $|\mathbf{E}(t)|$ are

$$\begin{aligned} \left|\mathbf{E}(t)\right|_{\ell_\infty} &= \sup_{0<t<\infty}\left\{\left|\mathbf{E}(t)\right|\right\} \\ \left|\mathbf{E}(t)\right|_{\ell_2} &= \lim_{T\to\infty}\sqrt{\frac{1}{T}\int_0^T \left|\mathbf{E}(t)\right|^2 dt} \end{aligned} \quad . \tag{13}$$

These formulas apply to arbitrary waveforms not just sinusoidal waveforms. Crest factor is defined as the ratio of the ℓ_∞ and ℓ_2 norms of the waveform.

$$\text{Crest Factor} = \frac{\left|\mathbf{E}(t)\right|_{\ell_\infty}}{\left|\mathbf{E}(t)\right|_{\ell_2}} \quad . \tag{14}$$

Formulas (13) and (14) are quite general and can be applied to arbitrary periodic waveforms, complex modulations, or signal environments made of many simultaneous signals. The mathematical limits are often replaced by a finite but long observation interval.

Many if not most texts on electromagnetic theory, particularly engineering texts after Harrington **[2]**, limit their treatments of time-varying fields to sinusoidal fields using complex phasor field notation as in (3). Our interest in instantaneous field magnitude requires the consideration of time-domain waveforms. Our principal interest is sinusoidal fields, but we will discuss more complicated fields in connection with broadband measurements below.

Peak Instantaneous Value

We shall evaluate the peak value defined in (5). We first change the order of operations as follows

$$\begin{aligned} E_{Peak} &= \max_{0<t<T}\left\{\left|\mathbf{E}(t)\right|\right\} \\ &= \max_{0<t<T}\sqrt{\left|\mathbf{E}(t)\right|^2} \\ &= \sqrt{\max_{0<t<T}\left|\mathbf{E}(t)\right|^2} \end{aligned} \tag{15}$$

which converts the problem to that of finding the maximum value of (7c). Now (7c) is the sum of a constant and a harmonic term $B(t)$ at twice the fundamental frequency.

$$\left|\mathbf{E}(t)\right|^2 = E_{rms}^2 + \frac{1}{2}B(t) \quad . \tag{16}$$

The harmonic term can be expressed as a phasor that is a sum of three phasors,

$$\begin{aligned} \underline{B}_{2\omega} &= \left(E_x^2\angle 2\phi_x\right)+\left(E_y^2\angle 2\phi_y\right)+\left(E_z^2\angle 2\phi_z\right) \\ &= \left(E_x^2 e^{j2\phi_x}\right)+\left(E_y^2 e^{j2\phi_y}\right)+\left(E_z^2 e^{j2\phi_z}\right) \\ &= \left|B_{2\omega}\right|\angle\phi_{2\omega} \end{aligned} \quad . \tag{17}$$

The subscripts are a reminder that the frequency of this phasor is 2ω. The real part, imaginary part, magnitude, and phase are given by

$$\begin{aligned} \underline{B}_{2\omega} = &\begin{pmatrix} E_x^2\cos 2\phi_x \\ +E_y^2\cos 2\phi_y \\ +E_z^2\cos 2\phi_z \end{pmatrix} \\ &+ j\begin{pmatrix} E_x^2\sin 2\phi_x \\ +E_y^2\sin 2\phi_y \\ +E_z^2\sin 2\phi_z \end{pmatrix} \end{aligned} \tag{18a}$$

where

$$\left|B_{2\omega}\right| = \left[\begin{pmatrix} E_x^2\cos 2\phi_x \\ +E_y^2\cos 2\phi_y \\ +E_z^2\cos 2\phi_z \end{pmatrix}^2 + \begin{pmatrix} E_x^2\sin 2\phi_x \\ +E_y^2\sin 2\phi_y \\ +E_z^2\sin 2\phi_z \end{pmatrix}^2\right]^{1/2} \tag{18b}$$

and

$$\phi_{2\omega} = \tan^{-1}\frac{\begin{pmatrix} E_x^2\sin 2\phi_x \\ +E_y^2\sin 2\phi_y \\ +E_z^2\sin 2\phi_z \end{pmatrix}}{\begin{pmatrix} E_x^2\cos 2\phi_x \\ +E_y^2\cos 2\phi_y \\ +E_z^2\cos 2\phi_z \end{pmatrix}} \quad . \tag{18c}$$

$B(t)$ is then

$$B(t) = \left|B_{2\omega}\right|\cos\left(\phi_{2\omega}+2\omega t\right) \tag{19}$$

In (16), as the cosine varies through a cycle, $B(t)$ alternately adds to or subtracts from the constant term. The constant term is positive. Consequently, the maximum occurs when the cosine is unity and $|B_{2\omega}|$ adds to the constant term. This happens when

$$2\omega t = -\phi_{2\omega} \pm 2n\pi \quad . \tag{20}$$

The peak instantaneous field is found by substituting the results obtained above into (15). The result is

$$E_{Peak} = \sqrt{E_{rms}^2 + \frac{1}{2}\left|B_{2\omega}\right|} \tag{21}$$

where $|B_{2\omega}|$ is given by (18). Two special cases are of interest.

Special Case 1: all component phases equal

A special case of interest occurs when the phase angles of the components, ϕ_x, ϕ_y, and ϕ_z are equal (modulo π). This case occurs, for example, if the field represents a linearly polarized wave. However, it should be emphasized that the field need not correspond to a wave. General, non-wave fields can have all field components in

phase too. An example is sinusoidal fields in a "single negative" or SNG metamaterial, specifically ENG or MNG material. Continuing, we obtain

$$\begin{aligned} |B_{2\omega}| &= E_x^2 + E_y^2 + E_z^2 \\ \phi_{2\omega} &= 2\phi_x = 2\phi_y = 2\phi_z \end{aligned} \tag{22a}$$

and

$$\begin{aligned} E_{Peak} &= \sqrt{2} E_{rms} \\ &= \sqrt{E_x^2 + E_y^2 + E_z^2} \end{aligned} \tag{22b}$$

and

$$\begin{aligned} |\mathbf{E}(t)| &= \sqrt{E_{Peak}^2 \frac{1+\cos(2\phi_x + 2\omega t)}{2}} \\ &= E_{Peak} |\cos(\phi_x + \omega t)| \end{aligned} . \tag{22c}$$

The instantaneous field magnitude is a rectified sinusoid at the fundamental frequency. This special case of components being in phase gives the largest possible ratio of E_{Peak} to E_{rms}, namely the square root of two.

Special Case 2: zero centroid

The second special case of interest occurs if $B(t) = B_{2\omega} = 0$. This happens when the centroid of the three phasors in (17) is zero.

$$0 = B_{2\omega} = E_x^2 e^{j2\phi_x} + E_y^2 e^{j2\phi_y} + E_z^2 e^{j2\phi_z} . \tag{23}$$

The three complex numbers are the squares of the electric field component phasors. Again it should be emphasized that the field need not correspond to a wave. General, non-wave fields can satisfy (23) too. For the zero-centroid case, we find

$$\begin{aligned} \underline{B}_{2\omega} &= 0 \\ |B_{2\omega}| &= 0 \\ \phi_{2\omega} &= \text{undefined} \\ E_{Peak} &= E_{rms} = \frac{1}{\sqrt{2}} \sqrt{E_x^2 + E_y^2 + E_z^2} \\ |\mathbf{E}(t)| &= E_{Peak} \text{ constant independent of } t \end{aligned} \tag{24}$$

The instantaneous field magnitude is constant, equal to both its peak and rms values. This special case of zero centroid gives the smallest possible ratio of E_{Peak} to E_{rms}, namely unity.

An example of a zero centroid occurs when the field represents a circularly polarized wave. Assume the coordinate system is rotated to align with the direction of wave travel and principle axes of the polarization ellipse. For example if the direction of wave travel is along the z axis, such that $E_z = 0$, $E_x = E_y$, and phase angles are in quadrature, $\phi_x = \phi_y \pm \pi/2$, then $2\phi_x = 2\phi_y \pm \pi$. (23) is thereby satisfied, and $E_{Peak} = E_{rms}$. So the peak and rms values of the field are equal.

Discussion

As seen above, the squared instantaneous magnitude $|\mathbf{E}(t)|^2$ of the electric field vector $\mathbf{E}(t)$ is a constant plus a second harmonic sinusoid. The ratio of peak instantaneous to rms value depends on the magnitude of the second harmonic term relative to the constant term. Special Cases 1 and 2 result in the maximum and minimum possible values of the second harmonic term and bound the crest factor or ratio of peak to rms of the magnitude of the electric (or magnetic) field between unity and the square root of two,

$$1 \le \frac{E_{Peak}}{E_{rms}} \le \sqrt{2} . \tag{25}$$

We conclude for sinusoidal fields, the crest factor or ratio of peak instantaneous to rms magnitude is not necessarily the square root of two. This is different from sinusoidal voltages or currents for which the ratio is exactly the square root of two.

Applications and Measurement of Fields

The instantaneous value of a field is important in disciplines concerned with failure mechanisms of media. In mechanical systems, one may be interested in material failure due to vibration. Similarly, in electrical systems, the breakdown of a material from RF voltage can be of interest. In such situations, it is often the peak instantaneous value of the field rather than its rms value that matters. The same may be true for athermal bioeffects as the relevant mechanisms become better understood from ongoing multidisciplinary research. In such applications the fields can be more complicated than the simple sinusoidal field considered here. In broadband applications, fields can be arbitrary periodic waveforms, complex modulations, or signal environments made of many simultaneous signals. The properties of sinusoidal fields are of interest in narrowband applications.

Some antenna modeling programs compute frequency domain quantities. Currents, voltages, and fields are sinusoidal in time and computed as phasors, one frequency at a time. Examples of such programs include moment method codes like *NEC2*, *NEC4*, *MiniNEC*, *FEKO*, *AWAS*, *WIPL-D*, and *HOBBIES*. When such programs report "total field" it is important to know what this means and what is being reported. In most cases, the "total field" is the rms value at a frequency of the magnitude of the field as given by (8). For some applications, however, one may want the peak instantaneous magnitude of a field. The peak value may be obtained by substituting the computed field phasors into (21).

When measuring fields, similar considerations apply. Certain EMF meters measure the combined field of all signals in a wide

Figure 1 — Extech model 480836 RF EMF strength meter. [Photo courtesy of Extech]

passband at once. The one shown in **Figure 1** is designed to sense fields from 50 MHz to 3.5 GHz. The "orange ball" sensor head houses an antenna array that has three perpendicular sensing electric field probes. Some sensors sense perpendicular magnetic field components too, by using Hall effect, "B-dot" devices, or crossed loop antennas, depending on frequency band. The electric or magnetic field components are processed in a series of steps that involve equalization or compensation for antenna frequency response, squaring (square-law diode rectification), summing and low-pass filtering to eliminate rectification harmonics. These steps are performed in analog circuitry. A/D conversion is then performed. In the pre-digital era, it was common to perform square roots in analog circuits by using an op amp with square-law feedback to the inverting input. Modern meters perform square root operations easily digitally. An operator may choose whether to display peak or rms values and an averaging interval. The final result is a peak or rms value of the field measured in the meter's bandwidth. With wideband meters, there is no assumption that a field is sinusoidal.

Sometimes, however, one wants to measure an individual signal, either in the near field or in the far field regions. **Figures 2, 3 and 4** show antenna arrays designed to measure the electric and magnetic field components of weak far field HF signals. These arrays are examples of "6-axis vector sensors." They are electrically larger than the sensor head shown in **Figure 1** to give the greater sensitivity needed to receive weak signals in the far field. **Figure 2** shows a Flam & Russell SuperCART array, **[3]**. **Figure 3A (left)** shows the EMVS array of M. Parent and W. Lee, **[4]**. **Figure 3B (right)** shows the author's *4nec2* model of the EMVS. **Figure 4** shows an array that uses six half loop antennas connected by hybrids to measure perpendicular electric field and magnetic field components, **[5]**. It is important when using such arrays to neutralize mutual coupling between elements. Perfect physical symmetry does not prevent mutual coupling because of proximity to the ground. The author has determined exact "manifold" corrections that can be applied after sampling. A multichannel SDR receiver connected to such an array can measure *I-Q* digital samples of the field components of an individual narrowband signal. For HF-band measurement a popular receiver is the Roke Manor Research MCDWR16. A pair of Kerberos 4-channel SDRs could also be used for sampling field components. The samples can be processed digitally by signal processing algorithms, **[6]**, to determine the properties of an incident signal, such as:

- the Poynting vector of the signal
- direction of arrival (azimuth and elevation angles)
- polarization (axial ratio, tilt, and sense)
- modulation properties.

For narrowband processing, an array covariance matrix is often computed from which the electric and magnetic field phasors may be calculated as if the field were sinusoidal. If only one signal is present in the filter passband, the crest factor of the magnitude of the electric (or magnetic) field determines the axial ratio of the signal polarization.

Figure 2 — Flam & Russell SuperCART array [Source: Bull and L.R. Burgess, 1990].

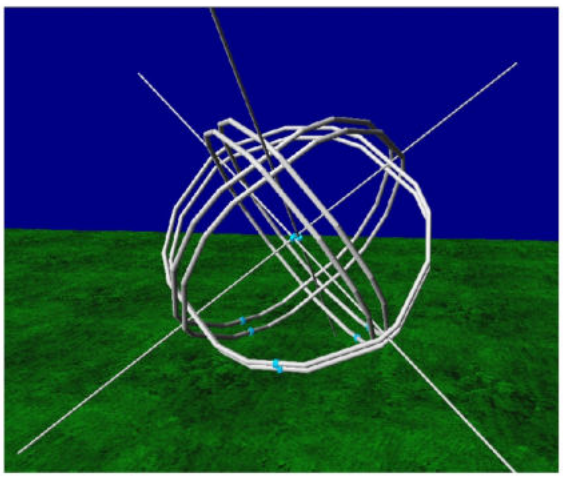

Figure 3 — 'A' (left) U.S. Navy EMVS, [Source: Parent and Lee, 2013]; 'B' (right) author's EMVS model.

Figure 4 — U.S. Navy HF vector-sensor array [Source: J.H. Meloling, *et al.*, 2016].

Historical Notes

In the 19th century, Peter Guthrie Tait, a classmate of James Clerk Maxwell,

tried to convince the young Maxwell to represent fields and potentials by using hyper-complex numbers called quaternions. Fortunately, a simpler representation of fields as vectors, developed later by Oliver Heaviside and Josiah Willard Gibbs, won out. A half century later a similar question arose: whether to represent monochromatic, single-frequency, time-harmonic fields as vectors whose components are complex or hyper-complex numbers, **[7] – [10]**. Another half century passed, and the modern representation of monochromatic fields as vectors having phasor components appeared, after WWII around 1960, **[2, pp. 15 – 16]**, **[11]**. Yet general treatments of the instantaneous properties of fields are scarce, **[12]**, **[13]**, except in works on nonlinear media, e.g. magnetic materials. Indeed, the results presented here have not been found in any text book. In modern times, steady-state frequency domain vector methods have been advanced by electrical engineers to facilitate practical calculations. Physicists meanwhile have worked largely in the time domain but shifted from vectors to coordinate-free methods, using tensors, differential geometry, and Clifford algebra or geometric algebra in order to facilitate abstract thinking about situations in which a system or observer moves or accelerates.

Conclusions

This paper addresses the crest factor of electric and magnetic vector fields. It is well known that the crest factor of arbitrary scalar waveforms can range from unity to infinity, and the crest factor of a sinusoidal waveform is the square root of two, **[1]**. The central result of this paper is equation (25). It was shown that for sinusoidal fields the crest factor of the magnitude of a field lies between unity and the square root of two. Moreover, every value in this range is achievable by, for example, a suitable selection of the axial ratio of elliptical wave polarization. Therefore, the statement that the crest factor of the magnitude of a sinusoidal field is the square root of two is a false oversimplification.

Acknowledgments

The author wishes to thank Dan Maguire, AC6LA, whose questions and numerical investigations motivated this paper.

Steve Stearns, K6OIK, started in ham radio while in high school at the height of the Heathkit era. He holds an FCC Amateur Extra and a commercial General Radio Operator license with Radar endorsement. He previously held Novice, Technician, and 1st Class Radiotelephone licenses. He studied electrical engineering at California State University Fullerton, the University of Southern California, and Stanford, specializing in electromagnetics, communication engineering and signal processing. Steve was a Technical Fellow of Northrop Grumman Corporation before retirement. He worked at Northrop Grumman's Electromagnetic Systems Laboratory in San Jose, California, where he led the development of advanced communication signal processing systems, circuits, antennas, and electromagnetic devices. Steve is Vice-President of the Foothills Amateur Radio Society, and served previously as Assistant Director of ARRL Pacific Division under Jim Maxwell, W6CF. He has over 80 professional publications and ten patents. Steve has received numerous awards for professional and community volunteer activities.

References

1 Wikipedia entry for *crest factor*: **https://en.wikipedia.org/wiki/Crest_factor**.
2 R.F. Harrington, *Time Harmonic Electromagnetic Fields*, 1st Ed., McGraw-Hill, 1961; 2nd Ed., IEEE Press-Wiley, 2001, chapter 1.
3 J.F. Bull and L.R. Burgess, "A Compact Antenna Array for Direction Finding in the HF Band," *Conf. on Tactical Communications*, Ft. Wayne, IN, Apr. 24-26, 1990.
4 W.W. Lee, M. Parent, and G. San Antonio, "High Frequency Vector Sensor Design and Testing," *2013 NRL Review*, pp. 154-156, June 2014.
5 J.H. Meloling, *et al.*, "A Vector-Sensing Antenna System," *IEEE Antennas and Propagation Magazine*, vol. 58, no. 6, pp. 57-63, Dec. 2016.
6 A. Nehorai and E. Paldi, "Electromagnetic Vector-Sensor Array Processing," chapter 65 in *The Digital Signal Processing Handbook*, 2nd Ed., CRC Press, 2010.
7 L. Silberstein, "Electromagnetische Grundgleichungen in bivectorielle Behandlung," *Annalen der Physik*, vol. 327, no. 3, pp. 579-586, 1907. Addendum in vol. 329, no. 14, pp. 783-784, 1907.
8 L. Silberstein, "Quaternionic Form of Relativity," *Phil. Mag.*, ser. 6, vol. 23, no. 137, pp. 790-809, May 1912.
9 H. Bateman, *The Mathematical Analysis of Electrical and Optical Wave-Motion*, Cambridge Univ. Press, 1915, chapter 1.
10 J.A. Stratton, *Electromagnetic Theory*, McGraw-Hill, 1941, p. 32.
11 R.M. Fano, L.J. Chu, and R.B. Adler, *Electromagnetic Fields, Energy, and Forces*, Wiley, 1960, pp. 317-320.
12 S. Ramo, J.R. Whinnery, and T. Van Duzer, *Fields and Waves in Communication Electronics*, Wiley, 1965, pp. 239-240.
13 Z. Popović and B.D. Popović, *Introductory Electromagnetics*, Prentice Hall, 2000, pp. 368-369.

Upcoming Conferences

GNU Radio Conference — Virtual GRCon20

September 14 – 18, 2020
www.gnuradio.org/grcon/grcon20

GRCon20 will be held September 14, 2020 online as a virtual event. The organizing team is hard at work to create a fun and interactive experience.

GNU Radio Conference (GRCon) is the annual conference for the GNU Radio project and community, and has established itself as one of the premier industry events for Software Radio. It is a week-long conference that includes high-quality technical content and valuable networking opportunities. GRCon is a venue that highlights design, implementation, and theory that has been practically applied in a useful way. GRCon attendees come from a large variety of backgrounds, including industry, academia, government, and hobbyists.

Call for Participation: We are looking for papers, presentations, posters, workshops, and lightning talks. Submit your work for presentation at **https://www.gnuradio.org/grcon/grcon20/submit**.

See website for details on submitting presentations, registration, and other ways you can be involved.

Eric P. Nichols, KL7AJ

3763 Lyle Ave., North Pole, AK 99705; **eric@alaskit.co**

Self-Paced Series of Essays in Electrical Engineering

It was the best of times, it was the worst of times
— Charles Dickens, A Tale of Two Cities.

Introduction

With the debut of the *QEX*-online edition, we gain the full ARRL membership in addition to our non-member printed edition subscribers as an audience. The membership profile boasts individuals from all walks of life — dentists, doctors, firefighters, police, nurses, mechanics, plumbers, entrepreneurs, bankers, and so on — and at all levels of technical expertise, not just engineers and technologists. This essay series introduces electrical engineering topics and concepts, and is aimed at technical neophytes, and at those with out-of-field expertise.

We begin this adventure as the entire world is in a state of chaos and uncertainty. In our present state of self-isolation and social distancing, countless of us ordinarily creative types were debating the wisdom, or even the very point, of embarking on any new projects. As so many others were shutting down and hunkering down, waiting for something encouraging to happen, it momentarily seemed a bit futile to make plans for anything involving the future, much less the present.

Yet, it was this very state of affairs that instigated and inspired this whole idea — to create an entire college level electrical engineering essay series using those very tools that have been proven the most useful during these times. As most conventional institutes of higher learning have been closed — or relegated to only an online presence — for the time being, what better time to fully test the latest educational ideas available to us. We might emerge from our "altered state of consciousness" with new, fairer ways of educating than ever before.

So, with the blessing of *QEX* magazine and ARRL, we shall embark on a complete self-paced essay series in electrical engineering, covering all the fundamental topics one would encounter in a "real" university-level electrical engineering (EE) course. Although — at least at this time — we cannot offer any degrees or other certifications, we will cover all the "classic" topics found in traditional EE courses. As further encouragement, every word we utter will be scrupulously peer-reviewed by our excellent and dedicated editor, Kai Siwiak — and we expect more experts in the field to chime in as we move along. Even when the world returns to a new normal, this essay series will be a valuable adjunct to a standard EE education. Your time dedicated to this series will not be wasted. And you can't beat the price!

We want this to be a highly interactive essay series. We strongly encourage you to ask us any pertinent questions you like, and we will do our best to answer your questions to your satisfaction. Please take your time to fully absorb all the concepts we present. Feel free to email me at **kl7aj@arrl.net**, with *EE Essay Series* in the subject line.

I trust this essay series will take us through these trying times together, in an enjoyable and productive manner.

As far as requisite adjunct materials are concerned, we highly recommend the *ARRL Handbook for Radio Communications*, and will refer to it frequently. The *Art of Electronics*, by Paul Horowitz, is also one of the best practical electronics texts ever written. We will recommend further literature on a regular basis as we proceed. You will also want a good scientific calculator, some notebooks — actual paper notebooks — and a reasonably decent computer, it doesn't have to be the latest and greatest. We will be using as much free engineering software as possible, and there is a vast selection available online.

The following *tentative* essay series outline will give you an idea of what to expect in the coming many months. If there are other topics you would like us to cover, we can add sections at any time, as this is, a work in progress. We can also adjust the overall pace according to your needs. May you have every success!

Essay Series Outline

Essay 1: Introduction

QEX: The ARRL Experimenters' Exchange was established in December of 1981 to promote advanced technical experimentation by addressing the needs of more technically minded radio amateurs and by playing a more active role in new communications and techniques. *QEX* articles tended to involve more advanced mathematics and technical analysis than the typical *QST* technical articles of the time. After several years, a number of *QST* readers made it known that they would be more interested in *QEX* if there were some kind of "on-ramp" to the advanced electrical engineering topics presented in *QEX*. This essay series is specifically designed to help hams and other interested parties make the transition to the electrical engineering mindset in a painless and enjoyable manner.

Essay 2: Setting up your home electrical engineering lab

Top quality test equipment has become so affordable that there is no excuse not to have a viable training lab in your ham shack or shop. We will present a shopping list for essential items for exploring EE topics. Since *QEX* stands for radio *Experimenters*, we will put a great deal of emphasis on constructing experiments to demonstrate the principles discussed in this essay series.

Essay 3: EE math the easy way

Electrical and electronic circuits are some of the best ways to demonstrate advanced mathematical concepts. Pure abstract math can be difficult for most people to grasp, but putting hardware to math concepts can bring them to life.

Essay 4: Ohms Law – Do you REALLY believe it?

Having taught electronics technology for many years, I have discovered that when students have a hard time troubleshooting or analyzing electronic circuits, it's almost always because they really don't understand or believe Ohm's Law! We will show how Ohms Law is NEVER violated, even in the most complex circuits, and is in fact aided and abetted by Kirchhoff's Laws and other principles.

Essay 5: Simultaneous Equations

We will take a brief tour into mathematics — with an air-tight promise to get right back into experimental electronics! Becoming thoroughly familiar with simultaneous equations will make *MESH* and *NODE* analysis a simple matter for the most part. Fortunately, most of our equations will be linear equations for at least half of this essay series.

Essay 6: Kirchhoff's Voltage Law (KVL)

Kirchhoff's Laws are among the most useful tools in the electrical engineer's arsenal, contrary to popular opinion, they actually make life simpler.

Essay 7: Kirchhoff's Current Law (KCL)

KVL and KCL are complements of each other, and we will demonstrate how any complex circuit can be solved with either KVL or KCL. In fact, we will demonstrate that there are always at least two ways to solve complex electrical network problem.

Essay 8: The Maximum Power Transfer Theorem

While not as concisely stated as KVL or KCL, the maximum power transfer theorem has profound implications for all that we do in radio work, or even electrical power transmission.

Essay 9: Energy Storage and Recovery

This is our first foray into ac electronics, and we will take a rather non-traditional approach to introducing concepts such as reactance and impedance — first working out problems without imaginary/complex numbers — and then showing how the imaginary number greatly simplifies matters.

Essay 10: Mechanics of Waves

The action of waves is a universal phenomenon, applicable to mechanical vibration, acoustics, radio propagation, and other physical realms. We will define standing wave ratio, reflection coefficient, and scattering parameters.

Essay 11: Filters

Filter design has been one of the most complex topics in all of electrical engineering. While digital filter design has greatly simplified the task for the average electrical engineer, the fundamental physics of filters will always apply.

Essay 12: Impedance Matching

While closely related to filters, impedance matching networks have different priorities.

Essay 13: Introduction to Active Devices

Active devices like diodes, transistors and vacuum tubes, are often misleadingly described as "non-Ohm's Law" devices. This is not correct. Even the most non-linear device follows Ohm's Law precisely. We simply need to recognize that the resistance and impedance is no longer constant.

Essay 14: Free Electrons and Plasmas

Basic plasma physics is an important part of modern electronics. But it's also part of very old electronics, such as in the vacuum tube. Understanding how electric currents behave in non-traditional conductors can give us new insights into the physical world.

Essay 15: Introduction to Digital Techniques

We have waited until we have fully explored traditional analog electronics before even touching digital electronics; that way digital methods will be a "snap." While there are nuances to digital methods that are somewhat tricky to grasp, the EE student who has a good grasp of the analog world can pick them up quickly.

Essay 16: Contrasting Combinational and Sequential Logic

Digital methods have traditionally been separated into combinational logic, which requires no memory, and sequential logic, which does require memory. The ancient dial telephone is a great example of sequential logic, and can give some useful insights into modern digital processing.

Essay 17: Digital Signal Processing

DSP technology has made tremendous strides in the past few years, and will continue to advance rapidly. However, DSP does not violate or make obsolete the underlying physics of radio or traditional analog circuits.

Summary and Wrap-up

Remember that this is a *tentative* outline. It is subject to change as we get feedback, and as we incorporate additional material.

Eric P. Nichols, KL7AJ, is a two-time recipient of the William Orr, W6SAI, Technical Writing Award. He has written numerous articles for QST and QEX magazine as well as four ARRL books, the latest being "Receiving Antennas for the Radio Amateur." Eric's latest focus is on encouraging experimentation on our two new LF bands on 2200 meters and 630 meters, heroically attempting to make up for lost time in catching up with our LF brethren across the pond.

Call for Papers: ARRL/TAPR Digital Communications Conference

Technical papers are solicited for presentation at the upcoming ARRL/TAPR Digital Communications Conference, set for September 11 – 13. Due to the coronavirus pandemic, this year's conference will be held online.

Papers will also be published in the Conference Proceedings. Authors do not need to participate in the conference to have their papers included in the Proceedings. The submission deadline is August 15, 2020.

Submit papers via email to Maty Weinberg, KB1EIB, at **maty@arrl.org**. Papers will be published exactly as submitted, and authors will retain all rights.

Make Summer Projects Simple with DX Engineering!

ICOM **New!**

IC-705 HF/VHF/UHF D-STAR All Mode Portable Transceiver

Icom's latest rig boasts the features of the IC-7300, IC-7610 and IC-9700 in a portable QRP package small enough to hold in one hand and fit inside a backpack. Features include SDR Direct Sampling technology; 4.3" color touch screen; and high-speed spectrum scope and waterfall display. This device has not been approved by the FCC and may not be offered for sale or lease, or be sold or leased, until approval of the FCC has been obtained. Check DXEngineering.com for availability.

MASTRANT ANTENNA GUYING

Guy Line Rope

Mastrant ropes are perfect for wire antennas, supporting Yagi booms and elements, as well as guying verticals and antenna masts. This non-conductive rope is made from synthetic fibers that won't stretch, collect moisture or suffer from UV degradation.

DX ENGINEERING

Wire Antennas

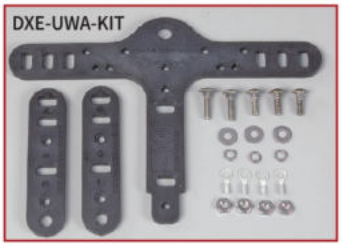

Choose from DX Engineering's versatile EZ-BUILD UWA Center T and End Insulator Kits that let you build virtually any wire antenna type; fan dipoles from EAntenna that use multiple parallel wires with spacers to allow each band dipole to remain separate; SOTABeams' portable and pre-assembled wire antenna kits; and an impressive selection from Alpha Delta, Buckmaster, Bushcomm, and others. **Enter "Wire Antenna" at DXEngineering.com.**

DX ENGINEERING

Coaxial Cable Assemblies

These low-loss cable assemblies are available in standard lengths with DX Engineering's revolutionary patented PL-259 connector. Use the online Custom Cable Builder at DXEngineering.com to build assemblies made to your exact specs. DX Engineering's coaxial cable is also available by the foot or in bulk spools.

DX ENGINEERING **New!**

Introducing Maxi-Core® 20 Baluns and Feedline Choke

DX Engineering ushers in an exciting era of upgraded RF performance across the 1.8 to 54 MHz frequency range with its four new Maxi-Core 20 baluns and one feedline choke. Building on the success of previous DX Engineering and Comtek units, the Maxi-Core 20 lineup—the culmination of years of research and development, equipment advancements and extensive testing— handles full-legal-power-plus and provides higher common mode impedance over the 160 through 6 meter bands. More of your signal gets to the antenna and you can hear more signals with less noise. Easy installation is provided by the optional DX Engineering Mounting Plate and Bracket Kit (DXE-MC20K-BRKT) or Wire Antenna Balun Mounting Bracket (DXE-WA-BMB). **Enter "Maxi-Core" at DXEngineering.com for applications and more details.**

DXE-MC20-1-1	High CMI 1:1 Current Choke Balun	**$123.99**
DXE-MC20-FC	High CMI 1:1 Feedline Choke, Line Isolator	**$137.99**
DXE-MC20-1-1T	High CMI 1:1 Current Choke Balun, Tuner Model	**$122.99**
DXE-MC20-C4-1	High CMI 4:1 Current Choke Balun	**$145.99**
DXE-MC20-V4-1	Low CMI 4:1 Voltage Balun	**$121.99**

DX ENGINEERING

Ladder Line

Good for both transmit and receive applications, DX Engineering ladder line is available in 300 and 450 ohm varieties. Both types feature high-quality stranded copper conductors, and will easily handle full legal limit power.

(((ON ALL BANDS)))
AN AMATEUR RADIO BLOG POWERED BY DX ENGINEERING

DX Engineering's Amateur Radio Blog for New and Experienced Hams.
Visit OnAllBands.com for information you can use to improve your on-air experience.

Free Standard Shipping for Orders Over $99. If your order, before tax, is over 99 bucks, then you won't spend a dime on shipping. (Additional special handling fees may be incurred for Hazardous Materials, Truck Freight, International Orders, Next Day Air, Oversize Shipments, etc.).

YAESU ICOM KENWOOD ALINCO RigExpert samlexamerica GATOR Cases iPortable

Showroom Staffing Hours:
9 am to 5 pm ET, Monday-Saturday

Ordering (via phone):
8:30 am to midnight ET, Monday-Friday
9 am to 5 pm ET, Weekends

Phone or e-mail Tech Support: 330-572-3200
8:30 am to 7 pm ET, Monday-Friday
9 am to 5 pm ET, Saturday
All Times Eastern I Country Code: +1
DXEngineering@DXEngineering.com

800-777-0703 | DXEngineering.com

DX 20 YEARS ENGINEERING

CELEBRATING 20 YEARS 2000-20

We're All Elmers Here! Ask us at: Elmer@DXEngineering.com
Email Support 24/7/365 at DXEngineering@DXEngineering.com

YouTube

ANALYZER OPTIONS

Pocket sized SARK antenna analyzers!

$239

SARK-110-ULM

The SARK-110-ULM is the entry-level model of the SARK-110 antenna analyzer series. This is a truly pocket-size device, so you can take it anywhere. The built-in battery lasts up to eight hours on a single charge. It features a graphical display and an intuitive user interface that makes it easy to operate.

The native measurement frequency range is between 0.1 and 160 MHz, but it operates up to 700 MHz with reduced performances. It has full vector measurement capability and accurately resolves the resistive, capacitive and inductive components of a load.

The functionality is not restricted to antenna analysis, but it is a multipurpose instrument featuring a Time Domain Reflectometer (TDR) mode which is intended for fault location and length determination in coaxial cables; as well as an RF signal generator. The analyzer is designed for standalone operation, but it can be controlled from your desktop using SARK Plots for Windows and from your tablet or smartphone using SARK Plots for Android through USB or short-range Bluetooth LE.

Typical applications include checking and tuning antennas, impedance matching, components test, cable fault location, measuring coaxial cable parameters, and cutting coaxial cables to precise electrical lengths. As a signal generator, it is ideal for receiver calibration, sensitivity tests, and signal tracing.

The above pricing for both units includes a 2 year warranty and free technical support!

$389

SARK-110

The SARK-110 antenna analyzer is a pocket-sized instrument that provides fast and accurate measurement of the vector impedance, VSWR, vector reflection coefficient, return loss and R-L-C.

Typical applications include checking and tuning antennas, impedance matching, component test, cable fault location, measuring coaxial cable losses and cutting coaxial cables to precise electrical lengths. The SARK-110 has full vector measurement capability and accurately resolves the resistive, capacitive and inductive components of a load.

The SARK-110 is intuitive and easy to use, and utilizes four operating modes: sweep mode, smith chart mode, single frequency mode and frequency domain reflectometer (cable test).

- **Pocket size and lightweight**
- **Solid aluminum metal case**
- **Intuitive and easy to use**
- **Four operating modes: sweep mode (antenna test), Smith chart mode, single frequency, and frequency domain reflectometer (cable test)**
- **Excellent accuracy over a broad range of impedances**
- **Resolves the sign of the impedance**
- **Manual and automatic positioning tracking markers**
- **Internal 2MB USB disk for the storage of measurements, screenshots, configuration and firmware update**
- **Export data in ZPLOTS compatible format for further analysis on the PC**
- **Lifetime free firmware upgrades available, open to community requested features**
- **Open source SDK including a device simulator for user applications development**

steppIR COMMUNICATION SYSTEMS

FOR DETAILS & SPECS ON THESE PRODUCTS, AND TO ORDER:

www.steppir.com 425-453-1910